Stony Brook University

Interannual Variability of U.S. West Coast and Alaska Winter Precipitation and Temperature

A Thesis Presented

by

Yilin Li

To

The Graduate School

In Partial fulfillment of the

Requirements

for the Degree of

Master of Science

In

Marine and Atmospheric Science

Stony Brook University

August 2007

Stony Brook University

The Graduate School

Yilin Li

We, the thesis committee for the above candidate for the
Master of Science degree,
hereby recommend acceptance of this thesis.

Dr. Sultan Hameed (Thesis Advisor)
Professor
Institute for Terrestrial and Planetary Atmospheres
School of Marine and Atmospheric Sciences

Dr. Minghua Zhang (Reader)
Professor and Director
Institute for Terrestrial and Planetary Atmospheres
School of Marine and Atmospheric Sciences

Dr. Nicole Riemer (Reader)
Assistant Professor
Institute for Terrestrial and Planetary Atmospheres
School of Marine and Atmospheric Sciences

This thesis is accepted by the Graduate School

Lawrence Martin
Dean of the Graduate School

Abstract of the Thesis

Interannual Variability of U.S. West Coast and Alaska Winter Precipitation and Temperature

by

Yilin Li

Master of Science
in

Marine and Atmospheric Science

Stony Brook University

2007

This study examines wintertime precipitation and temperature interannual variability in U.S. and Canada west coast, especially in Alaska and California. In the previous literature ENSO and PNA have been considered as the major teleconnection patterns which explain the variability of climate in this region. We take the Center Of Action (COA) approach, noting that changes in the intensities and locations of the Aleutian Low and the Hawaiian High pressure systems also significantly impact the climate in this region, often independently of the ENSO and PNA phenomena. The results presented in this thesis demonstrate that significantly greater portions of Interannual variance of winter temperature and precipitation can be explained by

including the contributions of the two COA in addition to ENSO and PNA. Physical mechanisms that explain the relationships between the COA and regional climate are explored by examining composite maps of large scale circulation fields using NCEP/NCAR Reanalysis data.

TABLE OF CONTENTS

List of Figures

List of Tables

Acknowledgments

I wish to thank Dr. Sultan Hameed, for his guidance, encouragement and patience during my thesis writing.

I am very grateful to Dr. Minghua Zhang, Dr. Nicole Riemer, Dr. Wuyin Lin.

I would like to thank Peng Cheng, Moguo Sun, Ling Wang, Xiaosong Yang, Joe Olson, Yanluan Lin, and fellow ITPA students.

The list doesn’t stop here and I deeply appreciate each of you who helped me during my stay in Stony Brook.

Chapter 1 Introduction

Climate variability in the U.S west coast has profound social and economic consequences, especially in the region along U.S. west coast. Droughts in late 1980s and early 1990s in California have resulted in a cost of approximately 3 billion dollars annually (Lott et al., 1997; Dettinger et al., 1998, Brown et al., 2004). Thus the understanding and predicting of the regional climate have been and continue to be of great research interests.

The U.S. west coast precipitation and temperature are shaped by atmosphere circulations and topography as well as teleconnection patterns. The bulk of precipitation occurs in the winter season with increasing magnitude towards north (Chen et al., 1996). On the other hand, summer precipitation in U.S. west coast is greatly suppressed by the northeastward shift of the Hawaiian High pressure system in the eastern Pacific which makes summer the driest season during any given year. Therefore, this study focuses on the U.S. and Canadian west coast wintertime climate variability and the underlying mechanisms.

Regarding of the processes modulating the U.S. west coast wintertime precipitation, previous studies focus on the influences of the El Niño-Southern Oscillation (ENSO) and the ocean-atmosphere interactions in the Pacific-North American Pattern (PNA) (Cayan et al., 1994; Haston et al., 1994; Haston et al., 1997; Mo et al., 1998; Brown et al., 2004.). It is argued that ENSO and PNA dominate the Pacific American coast by modifying planetary-scale atmospheric circulations and thus storm tracks (Mitchell and Blier, 1997).

However, ENSO and PNA by themselves can only explain a relatively small percentage of variance for the wintertime precipitation in the U.S. west coast, despite high correlations in certain areas. This study aims at studying the possibility that a

distinct increase in variance explained in U.S. west coast precipitation and temperature is possible by considering their relationships with the two atmospheric centers of action that dominate the circulation in the North Pacific, the Aleutian Low and the Hawaiian High, and perhaps new insights about the processes in large scale circulation that control regional climate can be generated. Several recent studies have illustrated these advantages of the COA approach, such as explaining the variability of cloud cover over the Western United States (Croke et al., 1999), the variations of zooplankton in the Gulf of Maine (Piontkovski and Hameed, 2002), the position of the Gulf stream northwall (Hameed and Piontkovski, 2004), the interannual variability of Saharan mineral dust transport over the Atlantic (Riemer et al., 2006), and the variability of wintertime Greenland Tipjet (Bakalian et. al., 2006).

Chapter 2 Data and Methods

2.1 Precipitation and Temperature data

Monthly precipitation and temperature data in U.S. and Canadian are obtained from Climate Research Unit, University of East Anglia, http://www.cru.uea.ac.uk/cru/data/hrg/cru_ts_2.10. This dataset is gridded on 0.5 latitude x 0.5 longitude. The methods of processing from station data into gridded data and the quality control methods have been described by Mitchell and Jones (2005). Considering the greater reliability of the data after the Second World War we present an analysis for 1951-2002.

2.2 Center Of Action indices

Monthly averaged gridded SLP data are used for calculating objective COA indices for the monthly averaged pressure, latitude and longitude of the Aleutian Low and the Hawaiian High pressure systems as described by (Hameed et al., 1995).

The definition of PNA index following Wallace and Gutzler (1981) is:
PNA = 0.25 * [Z(20N,160W) - Z(45N,165W) + Z(55N,115W) - Z(30N,85W)], where Z are standardized 500 mb geopotential height values. A high positive value of the monthly or seasonal PNA index indicates a strong positive PNA pattern; a highly negative value indicates a strong negative PNA pattern.

The PNA index used in this study is obtained from Climate Data Center, National Center for Environmental Prediction. To identify the PNA index, Rotated Principal Component Analysis (Barnston and Livezey, 1987) is applied to monthly mean standardized 500-mb height anomalies in the region 20°N-90°N. The RPCA procedure is superior to grid-point-based analyses in that PNA index is identified based on the entire

flow field, not just from height anomalies at select locations. http://www.cpc.ncep.noaa.gov/data/teledoc/telepatcalc.shtml

The Southern Oscillation Index (SOI) is defined as standardized anomaly of the Mean Sea Level Pressure difference between Tahiti and Darwin and is available from Australian Bureau of Meteorology.
http://www.bom.gov.au/climate/current/soihtm1.shtml

2.3 Methods

U.S. west coast wintertime precipitation and temperature variability are closely connected to large scale atmosphere circulations such as semi-permanent atmosphere centers of action. Winter values are calculated in three types of averages --- DJF, DJFM, and NDJFM to investigate the classification which can be best related to the COA in a given region.

Two rounds of linear regression analysis are explored. In the first round a multiple linear regression is calculated between the climate variable (temperature or precipitation) and all COA indices, PNA and SOI indices. We ignore any collinearity among the independent variables at this stage. The purpose is to identify regions where a significant amount of variation can be possibly explained by further study. Temperature and Precipitation indices averaged over the identified regions are calculated.

Next we identify the indices with large contributions that could be significant. Correlations are calculated among the indices. Only mutually independent indices are considered for further investigation. Thus, significant independent COA indices are identified for the second round of regression.

The second round of multiple linear regression is calculated between the regional average temperature or precipitation and the previously identified independent and significant indices only. The variance associated with each index designates the relative

importance of the index in modulating the regional variability. And the total variance gives confidence in relating and explaining these interannual variations.

Chapter 3 Winter Temperature Explained by COA indices

3.1 Introduction

The eight indices examined here are pressure, latitude, longitude of the Aleutian Low and Hawaiian High, PNA, and SOI index. Correlation maps show that these indices exhibit significant correlations with the wintertime temperature in the North American continent (figure 3.1). Canada and Alaska wintertime temperature is related with PNA, Aleutian Low pressure, and Aleutian Low longitude. The United States west coast and Nevada area wintertime temperature is connected with Aleutian Low latitude, Aleutian Low longitude, Aleutian Low pressure, Hawaiian High longitude, Hawaiian High pressure, and PNA.

A linear regression between wintertime temperature and all eight indices highlights the area where COA indices explain a significant percentage of variance (figure 3.2). Based on area where variance explained (r^2) is higher than 0.4 in the regression map (figure 3.2), three divisions are identified --- Alaska and Canada, United States west coast, and Nevada area.

3.2 Alaska and Canada

Based on the wintertime temperature regression map (figure 3.2), the Alaska and Canada region is the large area between 150°W-100°W and 45°N-65°N (figure 3.2 d). We have explored DJF, DJFM, and NDJFM averages as representative of winter. It is found that NDJFM and DJFM average give similar results and more of their variance can be explained than for DJF regarding to Alaska and Canada temperature (figure 3.2). Hereafter DJFM definition is adopted for winter temperature in Alaska and Canada area.

To understand the role of the centers of action in the interannual variability of wintertime temperature in Alaska and Canada, correlation between wintertime temperature and each COA index is calculated and examined. Statistically significant correlations occur in this region with PNA, Aleutian Low pressure, Aleutian Low longitude, Hawaiian High latitude, and SOI. But the largest contributions are from the PNA, Aleutian Low pressure, and Aleutian Low longitude (figure 3.3).

Two cases of temperature regression are explored for comparison. (1) Temperature regression with PNA and Aleutian Low longitude (figure 3.4); (2) Aleutian Low pressure and Aleutian Low longitude (figure 3.5). The spatial distributions are similar in two experiments. Compared with Aleutian Low pressure and Aleutian Low longitude regression, PNA and Aleutian Low longitude regression gives a better result in both intensity and range. In both regression experiments, variance values are highest along the North American coast beginning from Alaska all the way down to north California, and extend to the middle and western Canada. This special pattern of variance is considerably robust with the explained variance greater than or equal to 0.5 (figure 3.4 c).

To determine if the three COA indices used in the regression analysis are independent of each other, correlations among the three indices are shown in figure 3.6. Wintertime (DJFM) PNA and Aleutian Low pressure are highly correlated ($r = -0.90$) and not independent. Wintertime (DJFM) PNA and Aleutian Low longitude are also correlated though the correlation is not as high ($r = 0.64$). Correlation between wintertime (DJFM) Aleutian Low pressure and Aleutian Low longitude is -0.58.

Since neither pair of indices used in the above regression calculation is independent with each other, variance explained by each of the index only is examined. PNA is the dominant index connected with wintertime temperature in Alaska and Canada region, covering 150°W-100°W and 45°N-65°N with variances higher than 0.5 in most of the region (figure 3.7) and strongest intensity along the Canadian west coast (figure 3.7). Variance maps of Aleutian Low pressure resemble similar patterns as PNA with smaller

amplitude and range (figure 3.8). Aleutian Low longitude indicates variance only in middle Canada and part of northern Unite States (figure 3.9) with moderate amplitude.

3.3 United States west coast and Nevada area

The COA indices which are significantly related with United States west coast and Nevada area wintertime temperature include the PNA, Hawaiian high pressure, Aleutian Low longitude and Aleutian Low latitude (figure 3.10). While each index has connections with wintertime temperature in most of the area, each COA index exhibits focus on a specific region (figure 3.11). PNA has the strongest variance in west Oregon and northwest California; Hawaiian high pressure has the strongest variance in southwest Californian and Baja California; Aleutian Low longitude exhibits large variance in Oregon, Idaho, Nevada, and northeast California; and Aleutian Low latitude has considerable variance in southwest California, Baja California, and southwest Arizona.

Correlations among PNA, Hawaiian high pressure, Aleutian Low longitude, Aleutian Low latitude are shown in figure 3.12. It is found that wintertime (DJF) PNA and Aleutian Low longitude are correlated ($r=0.56$), and wintertime (DJF) Hawaiian high pressure and Aleutian Low latitude are also correlated ($r=0.55$). Two pairs of COA indices are found independent ($|r|<0.3$) and chosen for wintertime (DJF) temperature regression calculations. They are: (1) PNA and Hawaiian high pressure, (2) Aleutian Low longitude and Aleutian Low latitude.

Results of the two regressions are shown in figure 3.13. Regression with PNA and Hawaiian high pressure explains large variance along U.S. west coast and Baja California with the explained variance values greater than or equal to 0.5. On the other hand, regression with Aleutian Low longitude and Aleutian Low latitude explains large variance ($r2>0.5$) in Nevada, northeast California and southwest Idaho.

Based on variance distribution, two regions of interest are defined: (1) U.S. west coast, (2) Nevada area (figure 3.14). U.S. west coast is defined as the area enclosed by

the following six points: 125W, 45N; 122W, 45N; 122W, 39N; 115W, 33N; 115W, 30N; 125W, 30N. Nevada area is defined as a region enclosed by the following seven points: 122W, 44N; 117W, 44N; 117W, 42N; 114W, 42N; 114W, 37N; 117.2W, 37N; 122W,39N.

Results of area averaged regressions are shown in table 3.1. In recognition of the fact that the variance explained by PNA only is usually less than 0.4 even in its dominant areas, wintertime temperature variances explained by COA indices reach 0.65 in U.S. west coast and 0.59 in Nevada area. Dominant indices in U.S. west coast are PNA and Hawaiian high pressure, while dominant indices in Nevada area are Aleutian Low longitude and Aleutian Low latitude. We did similar calculations with DJFM and NDJFM winter averages. But the best regression results are found with the DJF averages for both U.S. west coast and Nevada.

The reconstructed time series (figure 3.14) from linear regression analysis captures the main characteristics of the observed data series, including the trend, frequency, and the extreme events, though the amplitude of the regression model is smaller. With high variances explained and reconstructed time series, it can be argued that the linear regression based on COA indices represents the U.S. west coast regional temperature variations well.

Chapter 4 Winter Precipitation Explained by COA indices

4.1 Introduction

Variance distributions of wintertime precipitation regression with the eight COA indices --- Aleutian Low latitude, Aleutian Low longitude, Aleutian Low pressure, Hawaiian High latitude, Hawaiian High longitude, Hawaiian High pressure, PNA, and SOI are shown in Fig. 4.1.. Four major regions in the North American continent can be identified in these maps: (1) Alaska; (2) West Canada and Columbia plateau; (3) California, and (4) Arizona, New Mexico and Mexico. While variance from PNA dominates in the southwest Canada region (figure 4.1 c), SOI gives the major contribution to variances in Arizona, New Mexico and Mexico (figure 4.1 d). Precipitation regression variances in Columbia plateau region stem from both PNA and Hawaiian High pressure. This study examines wintertime precipitation variances in two regions: Alaska and California.

4.2 Alaska

Four COA indices significantly related with wintertime Alaska precipitation are the Hawaiian High latitude, Aleutian Low pressure, Aleutian Low longitude, and PNA (figure 4.2). Wintertime (DJFM) correlations among these indices are shown in figure 4.3. With no independent pairs of indices, each index is examined specifically and a regression experiment with more than one index is not statistically justified. To inspect the influence of the different COA indices on a large area scenario, wintertime (DJFM) precipitation is averaged within 160°W-145°W, 60°N-70°N (figure 4.4). It is found that the best description of precipitation is given by Hawaiian High latitude which explains 39 percent of the variance for the area averaged wintertime (DJFM) precipitation in Alaska (table 4.1). Adding another variable to the Hawaiian High latitude does not show a clear increase in the explained variance. The Aleutian Low pressure and the PNA explain 0.17

and 0.15 of the variance respectively. The distribution of precipitation variance explained by Hawaiian High latitude is shown in figure 4.5, with highest values in the central and southwest of Alaska.

4.3 California

The COA indices connected significantly with wintertime (NDJFM) California precipitation include Hawaiian High pressure, Hawaiian High latitude, Hawaiian High longitude, and SOI (figure 4.6). With each index demonstrating correlations with precipitation through out the California region, Hawaiian High pressure and latitude dominate precipitation variability in northern California while the Hawaiian High longitude and SOI dominate it in the southern and Baja California.

Correlations among these four indices are shown in figure 4.7. The absolute values of correlation between wintertime (NDJFM) Hawaiian High pressure and other indices are less than 0.3 and considered to be independent with each other. Two pairs of indices are used for wintertime precipitation regression: (1) Hawaiian High pressure and latitude, (2) Hawaiian High pressure and longitude. Both cases show explained variances higher than 0.35 in a large portion of California, with case 1 giving better result in north California and case 2 better in south California (figure 4.8). Based on result from case 1, wintertime precipitation is averaged in California north of 35°N (figure 4.9). Area averaged regression results are shown in table 4.2, with the explained variance equal to 0.47 in NDJFM regression with Hawaiian high pressure and Hawaiian high latitude. Note that the dominant COA index in California north of 35°N is Hawaiian high pressure, yet Hawaiian high pressure itself can only explain 28% of the wintertime (NDJFM) precipitation variance, which is the highest value among variances explained by any single index in this region.

The regression with Hawaiian high pressure and Hawaiian high latitude captures the major patterns of wintertime observed precipitation variations from 1952 to 2001 (figure 4.10).

Chapter 5 Teleconnection mechanisms that support the statistical relationships between COA and climate variability

5.1 Introduction

In Chapters 3 and 4 we have found instances in which substantial amounts of regional temperature and precipitation in Alaska, Canada and the western coast of continental United States are explained by COA variations. In this chapter we present evidence that regional circulations of the atmosphere and the ocean are consistent with the empirically determined relationships. For this purpose we use the NCEP/NCAR Reanalysis monthly averaged fields of winds and geopotential heights together with NOAA extended sea surface temperature data. The method of composite analysis is used. For each regression result obtained in Chapters 3 and 4, the extremes of each COA index that increase temperature or precipitation were identified as equal to or greater than one standard deviation from the mean. Similarly the values of the index below one standard deviation from the mean were identified as contributing to a lowering of temperature or precipitation. The differences in composites for the years corresponding to the two sets of COA extremes were constructed using the NCEP/NCAR Reanalysis data. The years used for composite constructed in this manner are listed in the last two columns of Table 5.1 for each case.

5.2 Temperature in U.S. west coast

As shown in chapter 3, the dominant COA indices connected with U.S. west coast temperature variability are the PNA and Hawaiian High pressure. The best regression obtained was for the DJF season in this case and the same is used in making composites. As stated above, years when values of the COA index are higher or lower than one standard deviation are used but for PNA the threshold of 1.25 times the standard deviation were used.

Geopotential height composites indicate that high temperature anomaly in U.S. west coast is accompanied with an anomalous low geopotential height center in Pacific. Figure 5.1 shows the composites for 1000 mb geopotential heights but similar structure of geopotential height distribution is found in the middle and upper troposphere (not shown). The associated vector wind anomaly carries warm ocean air along the U.S. west coast (figure 5.2). Note that SST composite indicates warm anomalies exceeding $1^{o}C$ along the California coast and provide warm ocean air for U.S. west coastlines in wintertime (figure 5.3).

The sea surface temperatures along the western United States coast are influenced by the southward flowing California current which brings cooler waters from the north. The composites presented above suggest that the northward wind anomalies in this region seen in Figure 5.2 have the impact of slowing down the California current which results in the warm sea surface temperature anomalies along the coastline seen in Figure 5.3. Since long term California current data are not available, this hypothesis can be tested in an ocean-atmosphere global climate model.

5.3 Temperature in Alaska and Canada

Positive correlation is found (r=0.86) between wintertime (DJFM) PNA and temperature in Alaska and Canada. Composite 500mb Geopotential height map based on PNA phases demonstrate strong PNA pattern, as previous studies indicate (figure 5.4). Composite vector wind field associated with the PNA phase demonstrates inshore circulation in south edge of Alaska and west coast of British Columbia, as well as eastward wind toward British Columbia (figure 5.5, figure 5.6). At the same time, a warm belt of SST anomaly prevails along British Columbia all the way to U.S. west coast figure 5.7). As a result, the anomalous southerly wind brings anomalous warm ocean air into Alaska and Canada, contributing to a warmer winter in this region.

5.4 Precipitation in California

Precipitation regression with Hawaiian High pressure and latitude explains 47 percent of total variance in California NDJFM precipitation. Composite precipitation from the Arkin-Xie precipitation data set also indicates consistence with the phase of Hawaiian High pressure and latitude (figure 5.8). An anomalous low pressure centered northwest of California (figure 5.9) along with the anomalous wind field (figure 5.10) provides California area with enhanced water vapor source for precipitation. Composite meridional wind (figure 5.11) also indicates humidity source from Pacific Ocean, consistent with the high precipitation phase in California.

5.5 Precipitation in Alaska

Hawaiian High latitude explains 39 percent variance of the wintertime (DJFM) precipitation in Alaska (160°W-145°W, 60°N-70°N), as shown in table 4.1. A positive correlation of 0.63 is observed between wintertime (DJFM) Hawaiian High latitude and Alaska precipitation in the defined domain. Composite 850mb height displays an anomalous high pressure center in the Pacific Ocean and south of Alaska (figure 5.12). The associated vector wind and meridional wind (figure 5.13, figure 5.14) indicate that moist ocean air originating from southwest of Alaska contributes to a higher wintertime (DJFM) precipitation in Alaska.

Chapter 6 Conclusion and Discussion

The variability of wintertime temperature and precipitation in several regions of the North American continent is connected with atmospheric centers of action as well as with PNA teleconnection and ENSO tropical influences. Conventionally, ENSO and the PNA have been considered the dominant modulators of regional variability in this region. The results presented in this work has demonstrated that the inclusion of the Aleutian Low and the Hawaiian High explains significantly increased variance in both temperature and precipitation variability. Furthermore, it is not only the fluctuations of the pressures of these centers but shifts in their latitude and longitude positions can also significantly impact the distribution of temperature and precipitation from year to year.

Along the U.S. west coast, essential contributing indices for wintertime temperature variability are PNA and Hawaiian High pressure, explaining 0.65 of the total variance. Note that PNA alone can only explain 0.38 of the variance of wintertime precipitation along the U.S. west coast. Composite circulation maps show that the positive SST anomaly along the coast reaching up to $1^{o}C$ gives rise to warm ocean air which is transported inshore along the coast by anomalous meridional winds, contributing to the above normal wintertime temperature along the U.S. west coast.

In Alaska and west Canada (British Columbia, and Alberta province), PNA is the major index connected with wintertime temperature variability, with variance explained by PNA higher than 0.5 in most of the Alaska & Canada region. High winter temperatures in Alaska & Canada region are introduced by the inshore wind and above normal SST west of Canada associated with the PNA phase. Regarding wintertime temperature variability, SOI index solely dominates the Baja California, south Arizona, south New Mexico, and Mexico region.

Regression analysis shows that Hawaiian High pressure and latitude together explain 0.47 of the total variance in wintertime California precipitation. Above normal moisture is transported to California by the anomalous meridional winds associated with the shifts in the Hawaiian High. The along coast mountain chain uplifts the moist air mass, resulting in above normal precipitation in California.

Regression analysis also shows that Hawaiian high latitude position is the main influence contributing to the variance explained in Alaska wintertime precipitation. Hawaiian high latitude itself explains 0.39 in the total variance of Alaska wintertime precipitation. Composite circulation maps show that when Hawaiian High moves northward, anomalous low level wind associated with Hawaiian High brings ocean air form southwest to Alaska and lead to increased precipitation in Alaska.

The role of each COA and its pressure, latitude or longitude variables plays in the temperature and precipitation variability in Alaska and U.S. west coast is subject to further examination. The Aleutian Low and the Hawaiian are signatures of stationary waves in the atmospheric general circulation. How their variations feedback with each other, with PNA and the SOI and co-influence temperature and precipitation variability via large scale circulation and teleconnections is a question that needs further inspection. The suggested mechanisms we have presented using NCEP/NCAR Reanalysis data show consistency between the large scale circulation and regional impacts associated with the shifts in the COA, in which cause and effect are difficult to separate. Numerical experiments in coupled ocean-atmosphere General Circulation Models can possibly provide further understanding. But first we should investigate if the GCM we use correctly simulates the seasonal and interannual variations of the centers of action.

Correlations between COA indices (DJF)

	H_SLP	H_LON	H_LAT	A_SLP	A_LON	A_LAT	SOI	PNA
H_SLP	\\\\							
H_LON		\\\\						
H_LAT		0.62	\\\\					
A_SLP				\\\\				
A_LON		-0.40	-0.55	-0.55	\\\\			
A_LAT	0.55	-0.61				\\\\		
SOI		0.67	0.50	0.38	-0.55		\\\\	
PNA			-0.33	-0.89	0.56		-0.37	\\\\

Correlation between COA indices (DJFM)

	H_SLP	H_LON	H_LAT	A_SLP	A_LON	A_LAT	SOI	PNA
H_SLP	\\\\							
H_LON		\\\\						
H_LAT		0.63	\\\\					
A_SLP			0.41	\\\\				
A_LON		-0.38	-0.52	-0.58	\\\\			
A_LAT	0.58	-0.46				\\\\		
SOI		0.68	0.54	0.48	-0.52		\\\\	
PNA			-0.48	-0.90	0.64		-0.55	\\\\

Correlation between COA indices (NDJFM)

	H_SLP	H_LON	H_LAT	A_SLP	A_LON	A_LAT	SOI	PNA
H_SLP	\\\\							
H_LON		\\\\						
H_LAT		0.58	\\\\					
A_SLP			0.38	\\\\				
A_LON		-0.38	-0.37	-0.42	\\\\			
A_LAT	0.57	-0.46				\\\\		
SOI		0.70	0.50	0.49	-0.45		\\\\	
PNA			-0.44	-0.88	0.53		-0.51	\\\\

Table 3.1: Correlations among indices for DJF, DJFM, and NDJFM. Data from 1952 to 2001 are used.

Region	Indices	Variance		
		DJF	DJFM	NDJFM
U.S. west coast	**PNA and Hawaiian high pressure**	**0.65**	0.60	0.47
U.S. west coast	Aleutian Low longitude and Aleutian Low latitude	0.53	0.39	0.21
U.S. west coast	PNA	0.38	0.33	0.20
U.S. west coast	Hawaiian high pressure	0.26	0.33	0.24
U.S. west coast	Aleutian Low longitude	0.25	0.16	0.06
U.S. west coast	Aleutian Low latitude	0.23	0.22	0.14
Nevada area	**Aleutian Low longitude and Aleutian Low latitude**	**0.59**	0.41	0.22
Nevada area	PNA and Hawaiian high pressure	0.38	0.43	0.28
Nevada area	Aleutian Low longitude	0.39	0.21	0.09
Nevada area	Aleutian Low latitude	0.15	0.19	0.12
Nevada area	PNA	0.20	0.21	0.08
Nevada area	Hawaiian high pressure	0.18	0.25	0.18

Table 3.2: Variances from area averaged wintertime U.S. west coast and Nevada temperature regression and from single indices only.

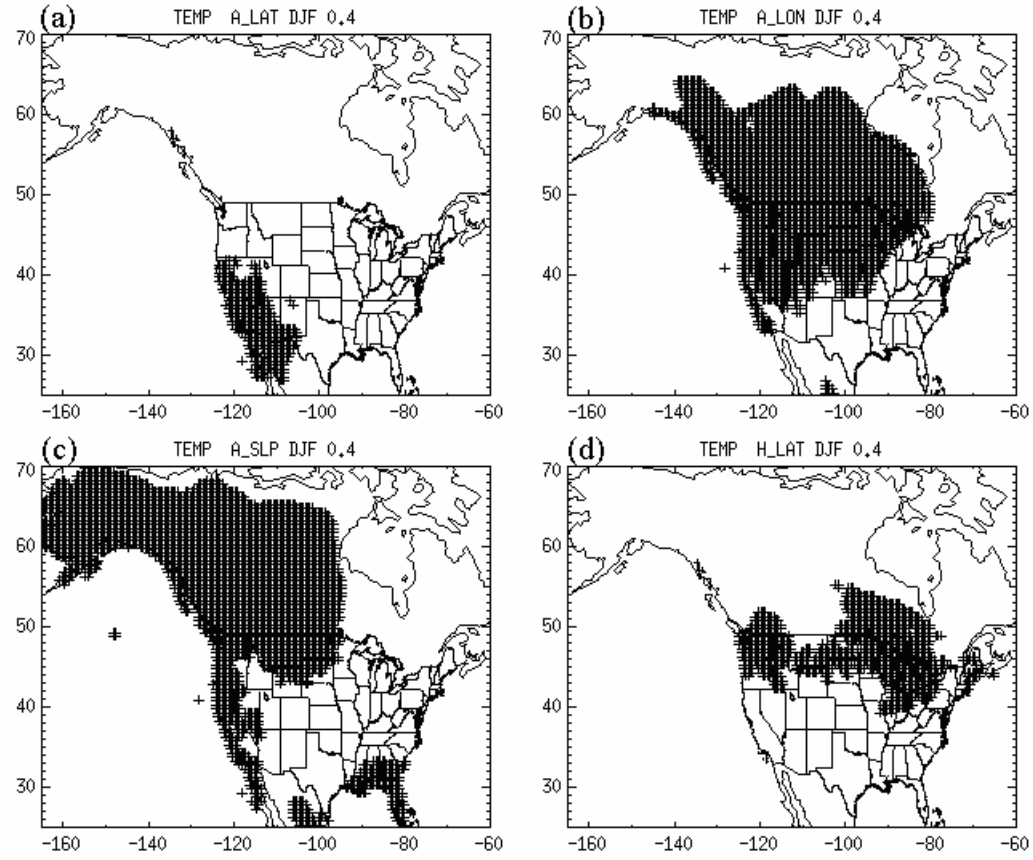

Figure 3.1: Correlations maps between North American wintertime (DJF) temperature and COA indices. Grid points where absolute value of the correlation coefficient are higher than 0.4 are marked. COA indices including: (a) Aleutian Low latitude, (b) Aleutian Low longitude, (c) Aleutian Low sea level pressure, (d) Hawaiian High latitude. To be continued.

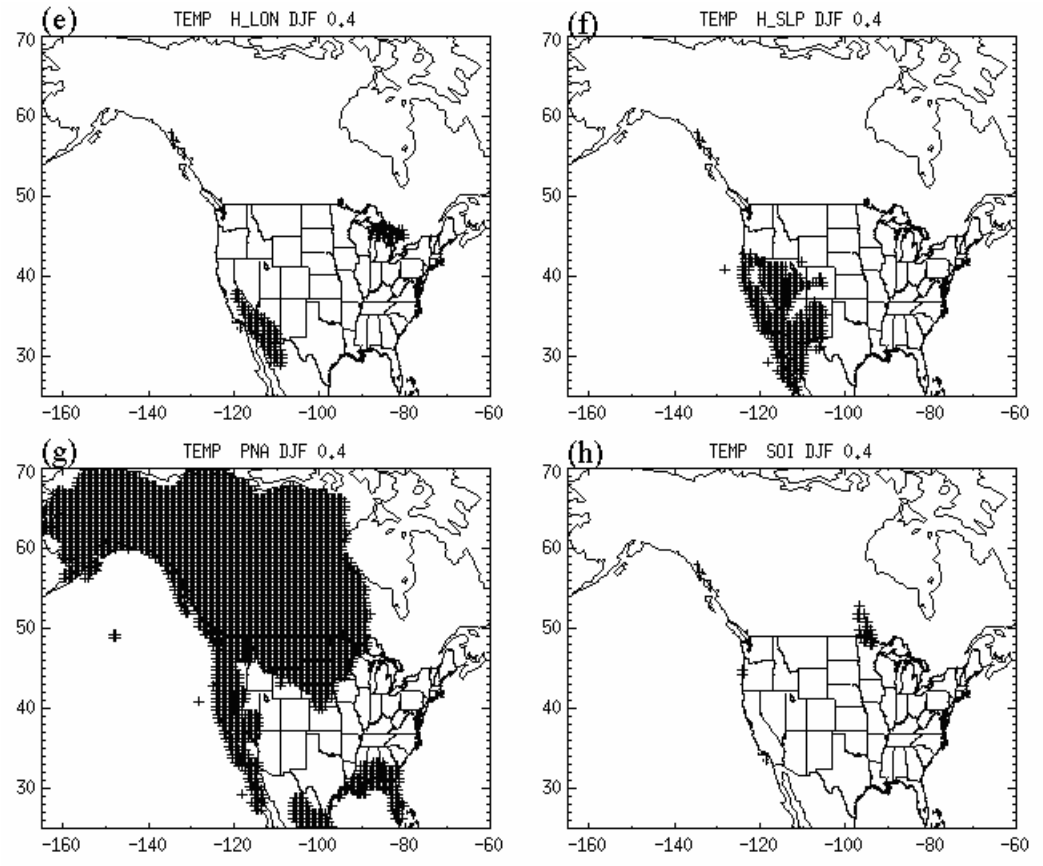

Figure 3.1: Continued. Correlations maps between North American wintertime (DJF) temperature and COA indices. Grid points where absolute value of the correlation coefficient are higher than 0.4 are marked. COA indices including: (e) Hawaiian High longitude, (f) Hawaiian High sea level pressure, (g) PNA, and (h) SOI.

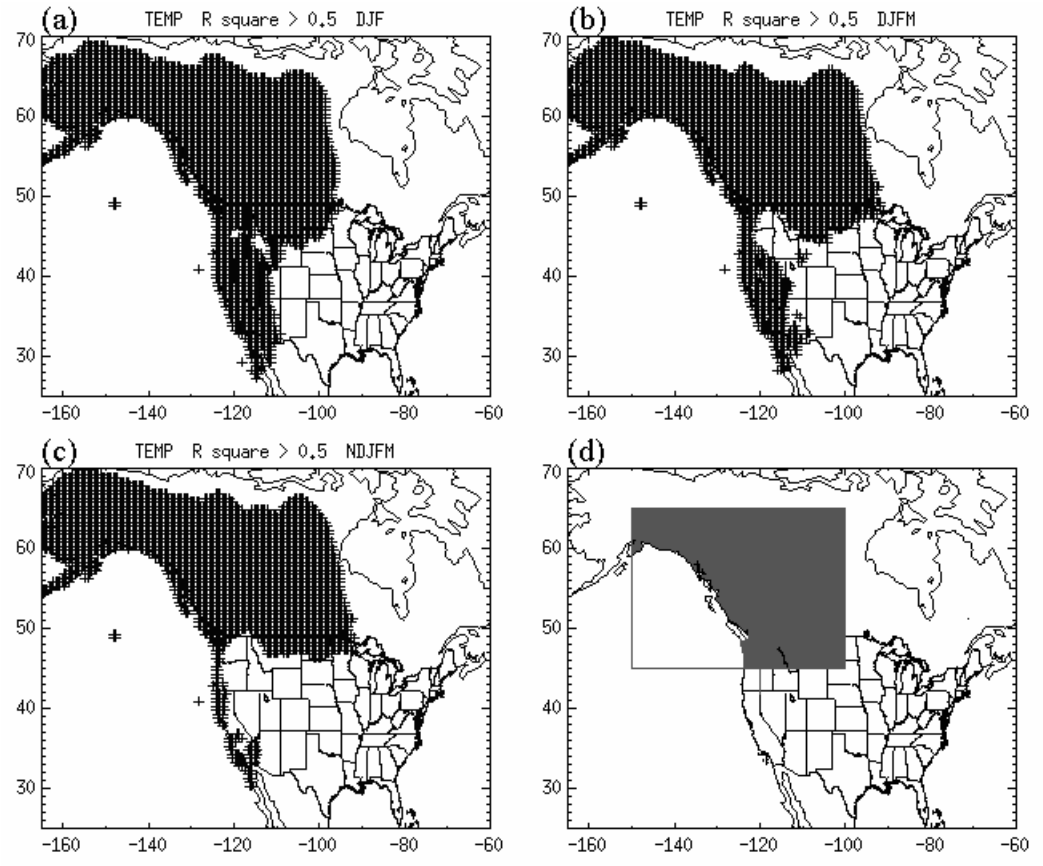

Figure 3.2: (a) North American wintertime (DJF) temperature regression with COA indices including Aleutian Low latitude, longitude, pressure, Hawaiian High latitude, longitude, pressure, PNA, and SOI index. (b) same as (a) but wintertime is averaged on DJFM. (c) same as (a) but wintertime is averaged on NDJFM. For (a)-(c), variance values higher than 0.5 are marked . (d) Alaska and Canada region is defined as the shadowed area within the box.

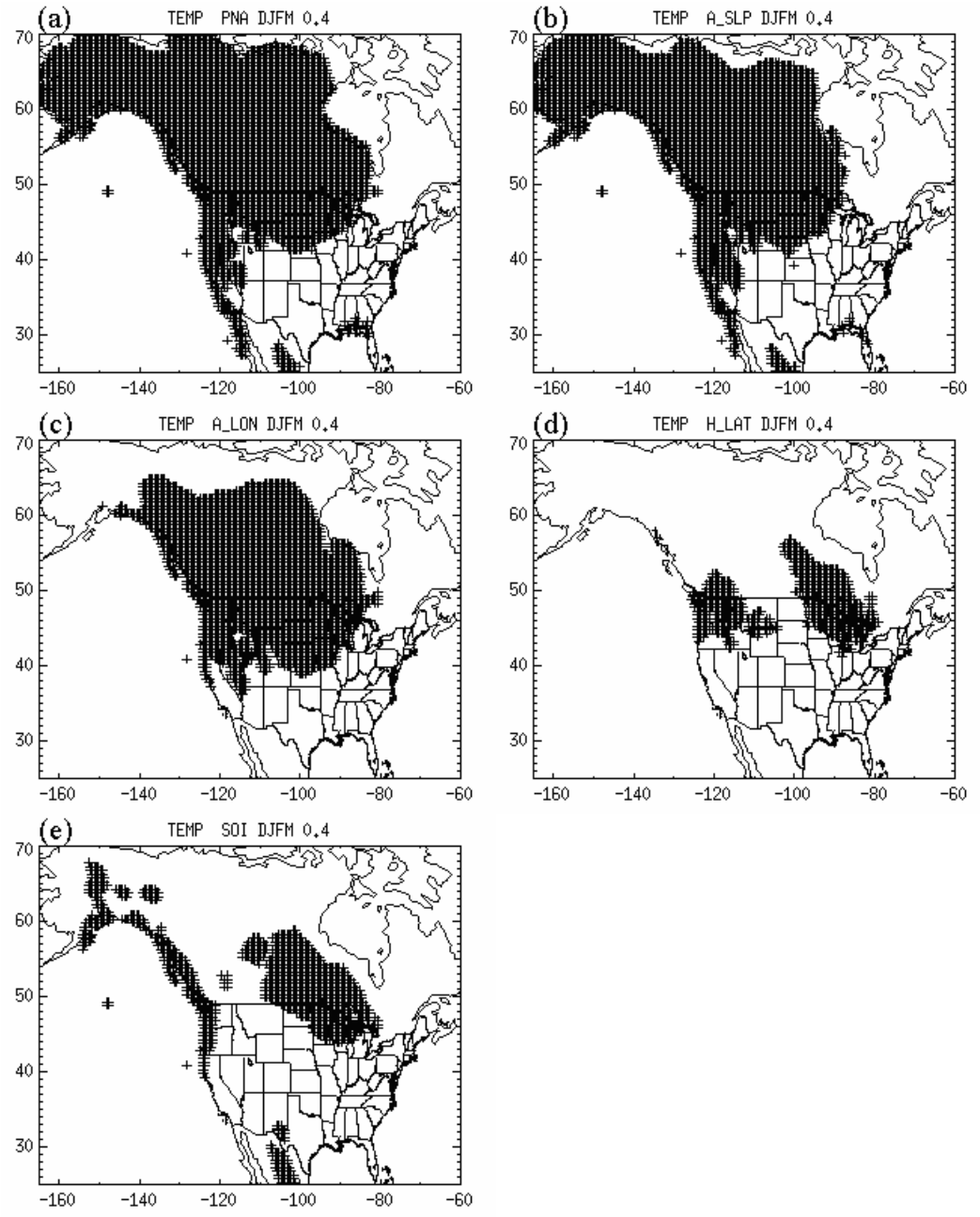

Figure 3.3: Pearson's correlation between North American wintertime (DJFM) temperature and (a) PNA, (b) Aleutian Low pressure, (c) Aleutian Low longitude, (d) Hawaiian High latitude, (e) SOI. Absolute correlation values higher than 0.4 are marked.

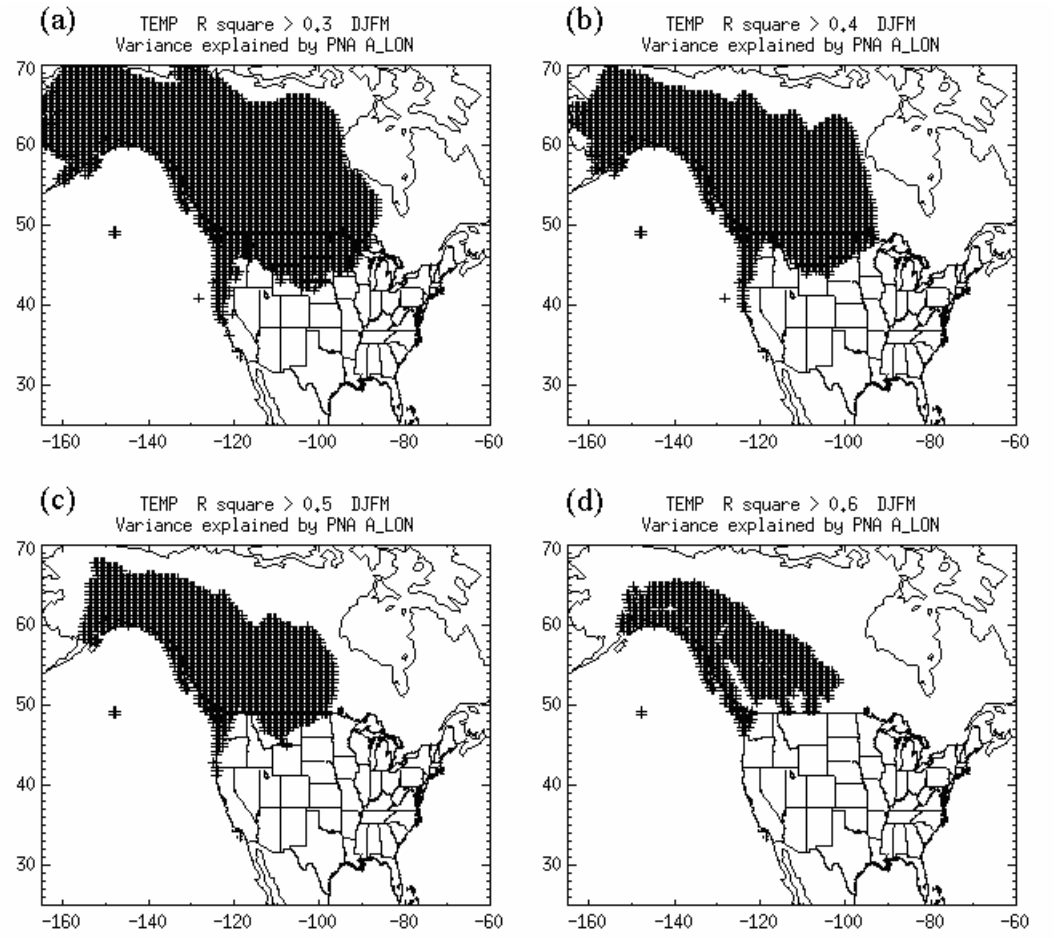

Figure 3.4: North American wintertime (DJFM) temperature regression with PNA and Aleutian Low longitude. The grid points where the variance explained are higher than a threshold of (a) 0.3, (b) 0.4, (c) 0.5, (d) 0.6. are marked.

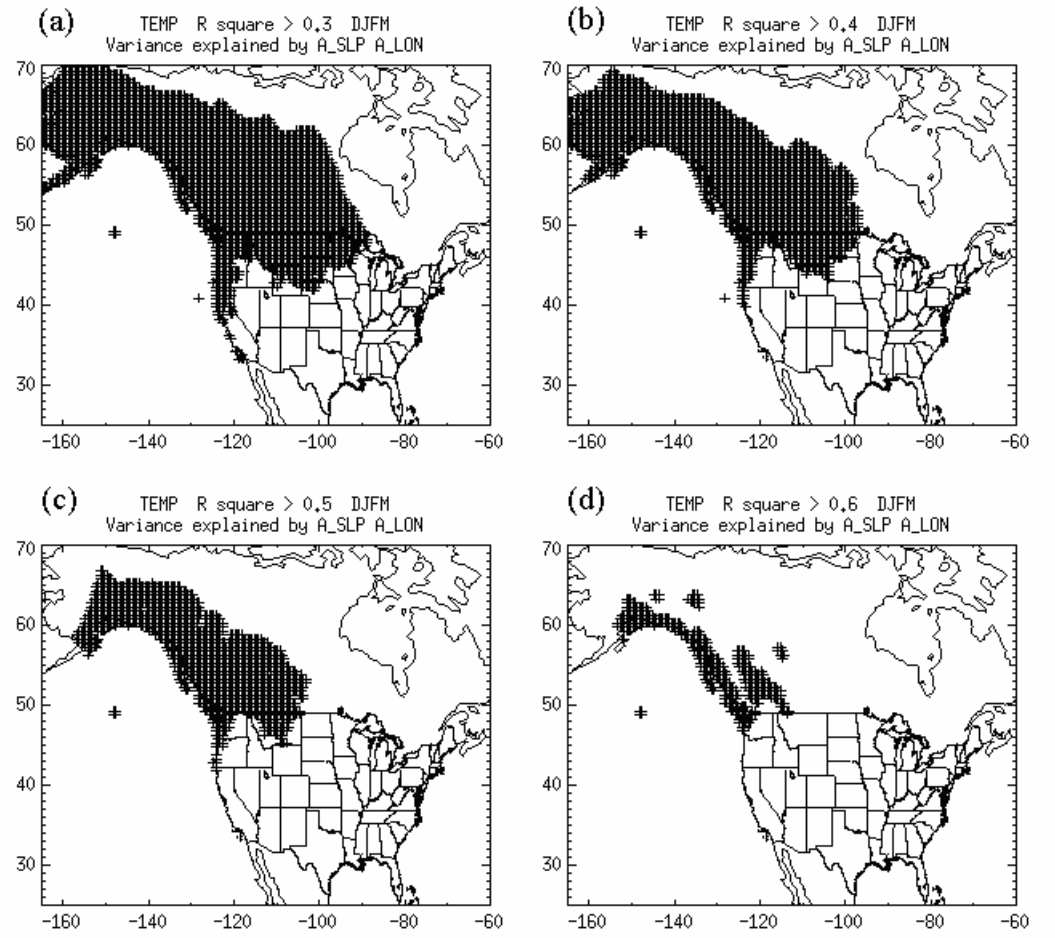

Figure 3.5: North American wintertime (DJFM) temperature regression with Aleutian Low pressure and Aleutian Low longitude. The grid points where the variance explained are higher than a threshold of (a) 0.3, (b) 0.4, (c) 0.5, (d) 0.6. are marked.

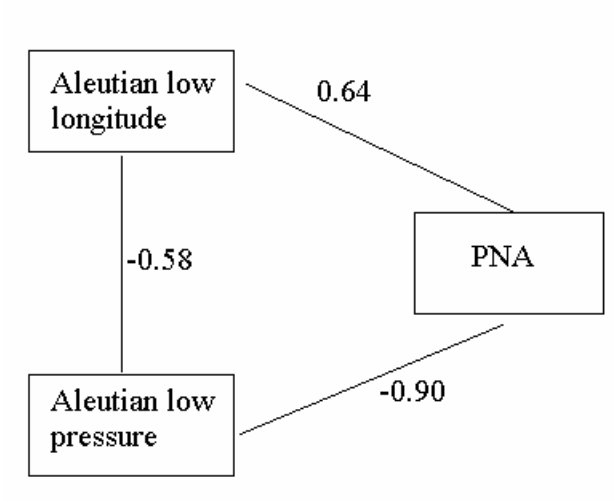

Figure 3.6: Pearson's correlation coefficients between wintertime (DJFM) PNA, Aleutian Low longitude, and Aleutian Low pressure.

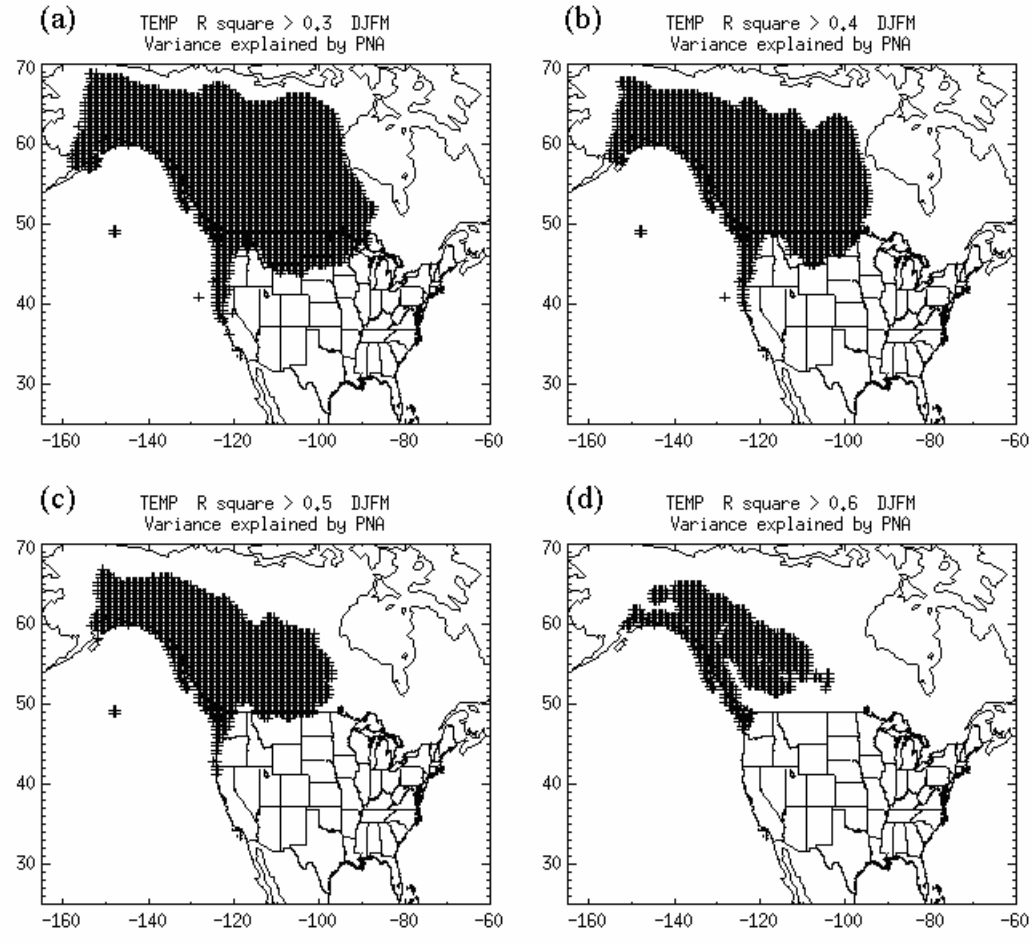

Figure 3.7: Variance of North American wintertime (DJFM) temperature explained by PNA only. The grid points where the variances are higher than a threshold of (a) 0.3, (b) 0.4, (c) 0.5, (d) 0.6 are marked.

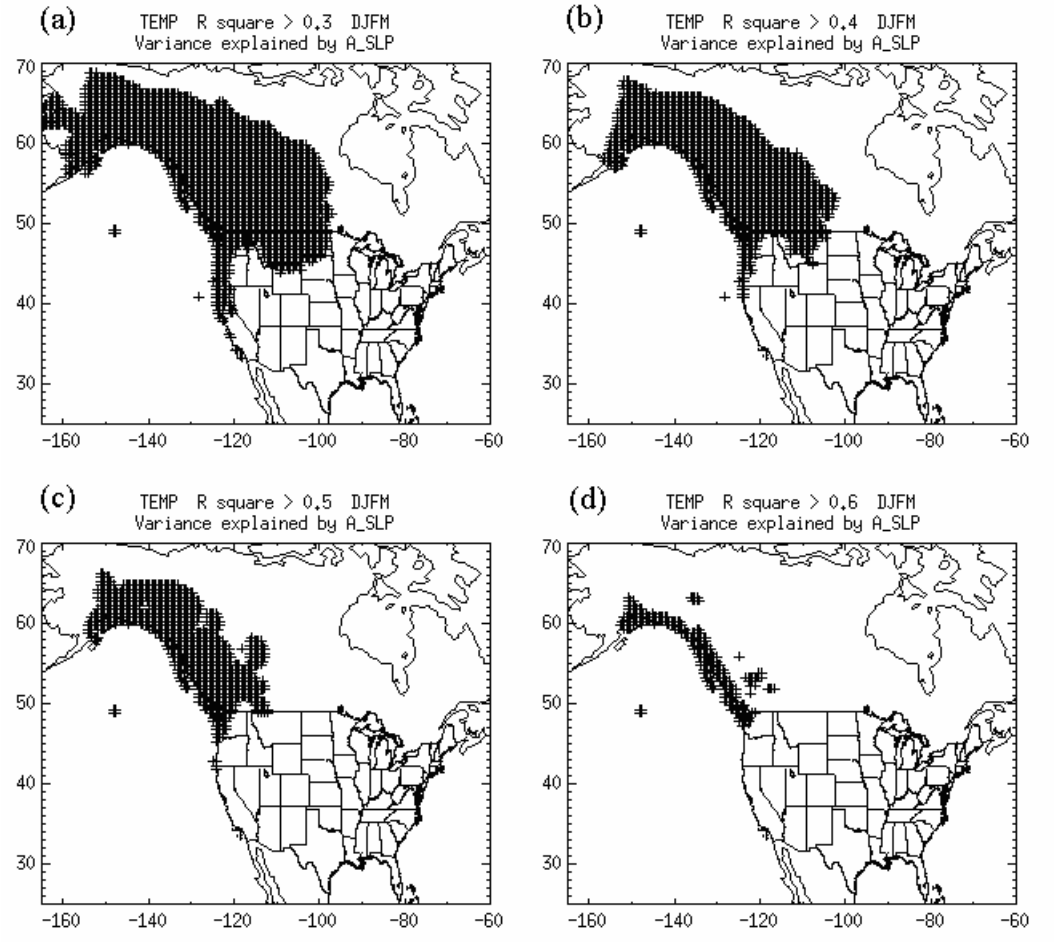

Figure 3.8: Variance of North American wintertime (DJFM) temperature explained by Aleutian Low pressure only. The grid points where the variances are higher than a threshold of (a) 0.3, (b) 0.4, (c) 0.5, (d) 0.6 are marked.

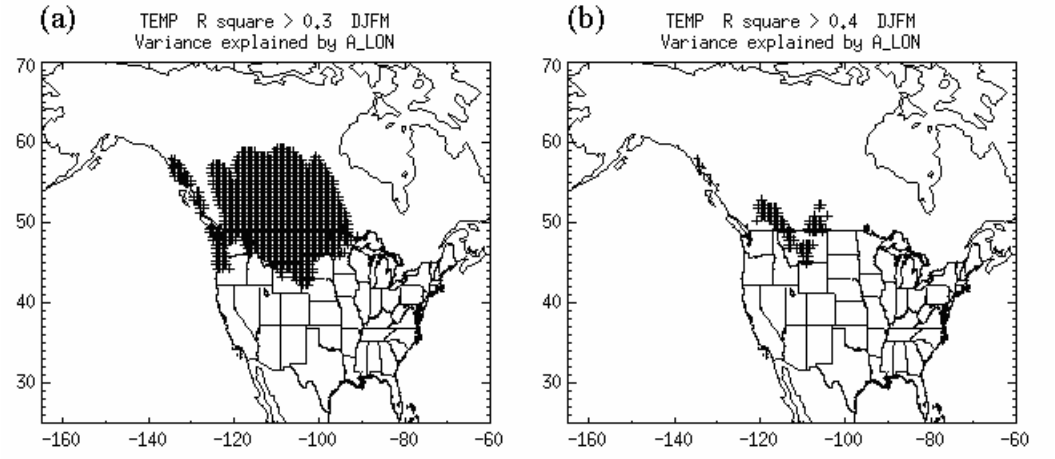

Figure 3.9: Variance of North American wintertime (DJFM) temperature explained by Aleutian Low longitude only. The grid points where the variances are higher than a threshold of (a) 0.3, (b) 0.4 are marked.

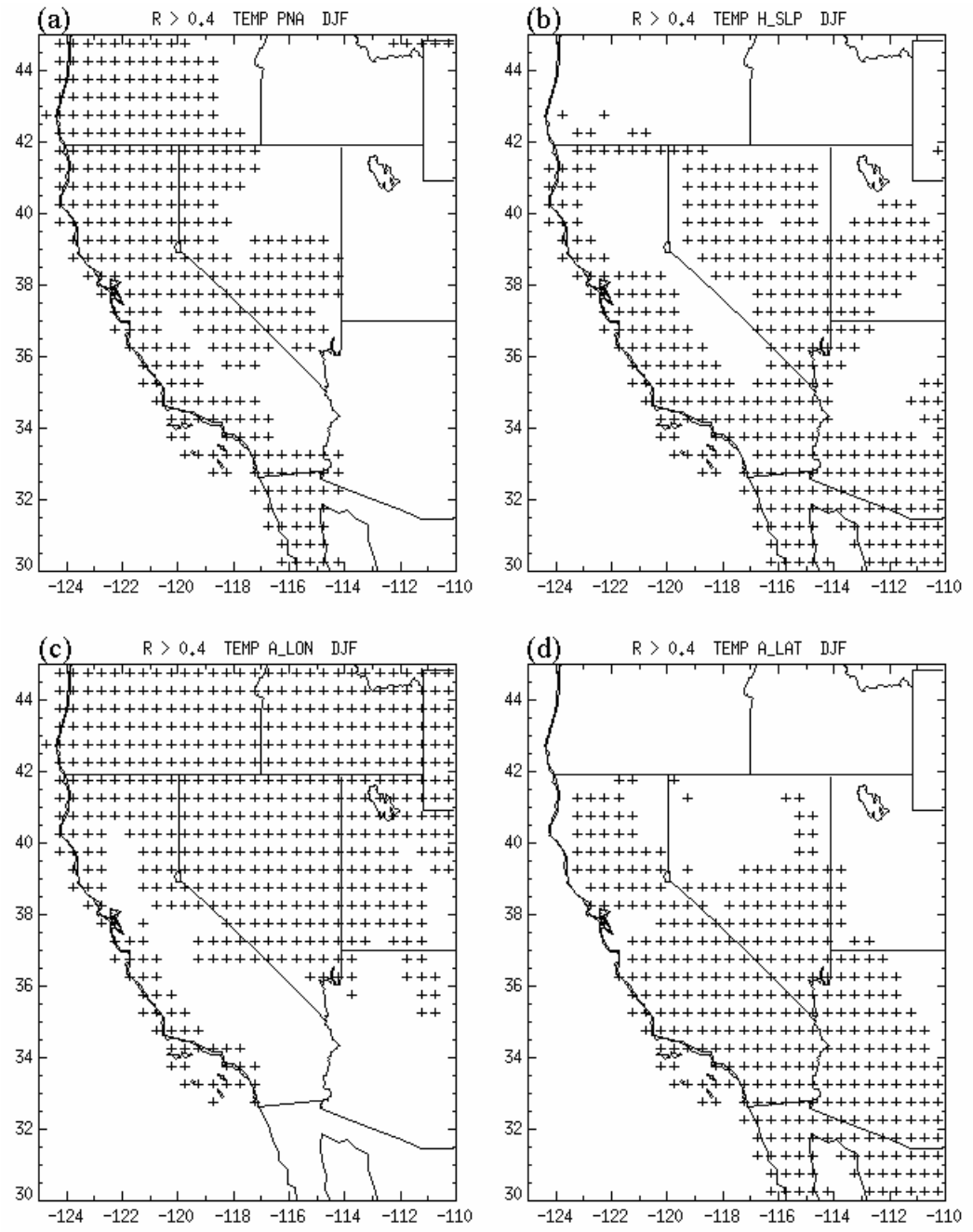

Figure 3.10: Correlations maps between U.S. west coast wintertime (DJF) temperature and COA indices. Grid points where absolute value of correlation coefficient higher than 0.4 are marked with cross. COA indices including: (a) PNA, (b) Hawaiian High pressure, (c) Aleutian Low longitude, (d) Aleutian Low latitude.

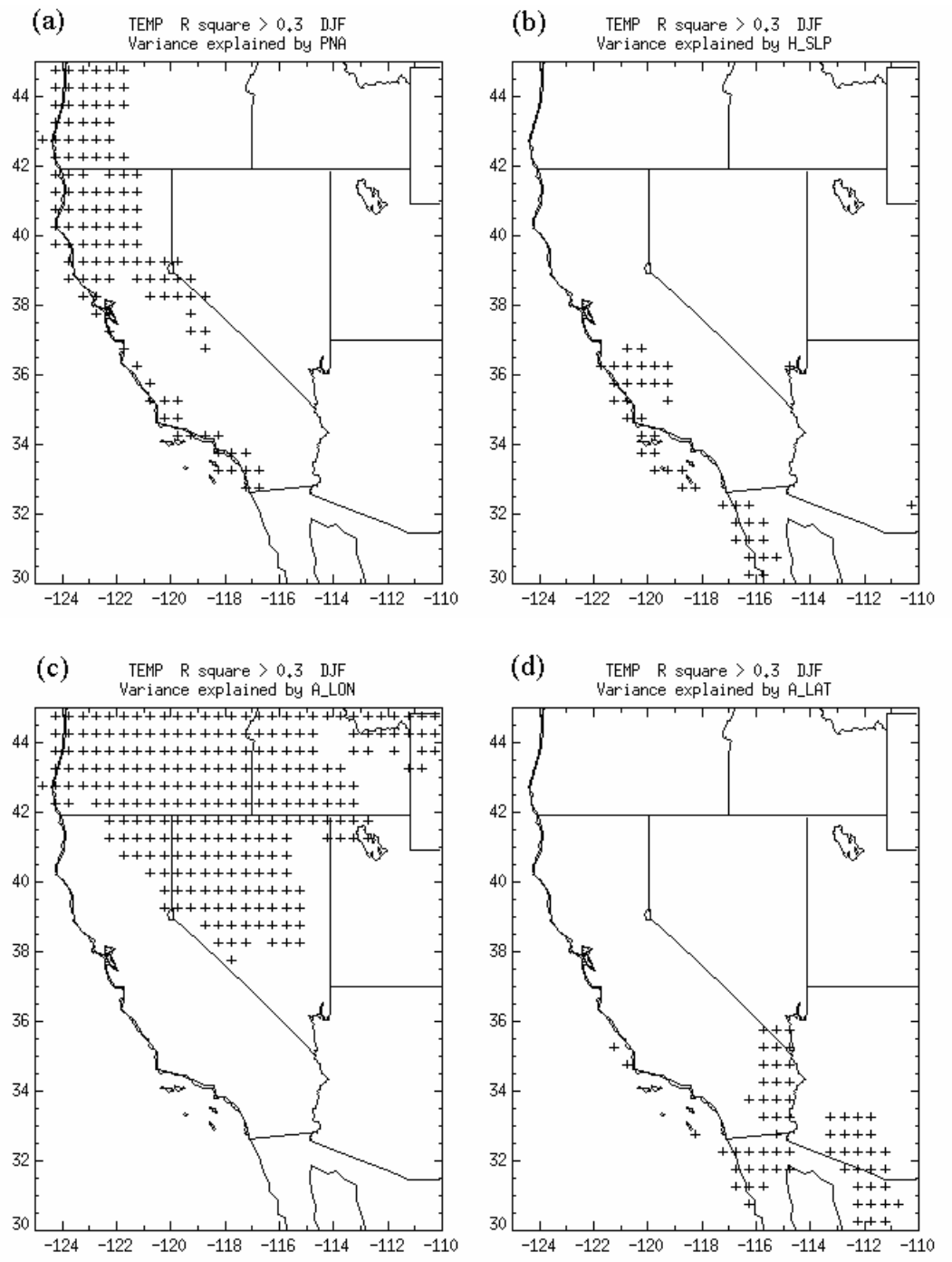

Figure 3.11: Variance of U.S. west coast wintertime (DJFM) temperature explained by (a) PNA, (b) Hawaiian High pressure, (c) Aleutian Low longitude, (d) Aleutian Low latitude.

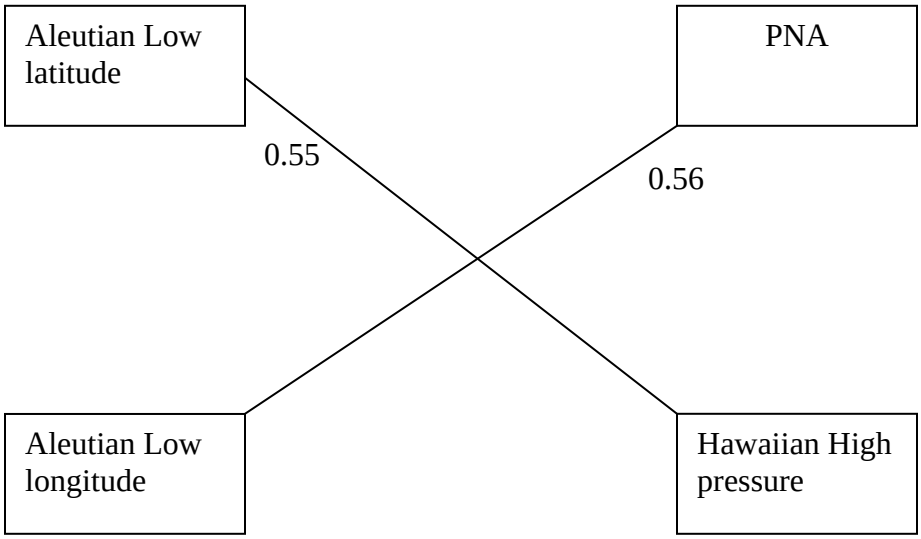

Figure 3.12: Pearson's correlation coefficients between wintertime (DJF) PNA, Aleutian Low longitude, and Aleutian Low latitude, and Hawaiian High pressure.

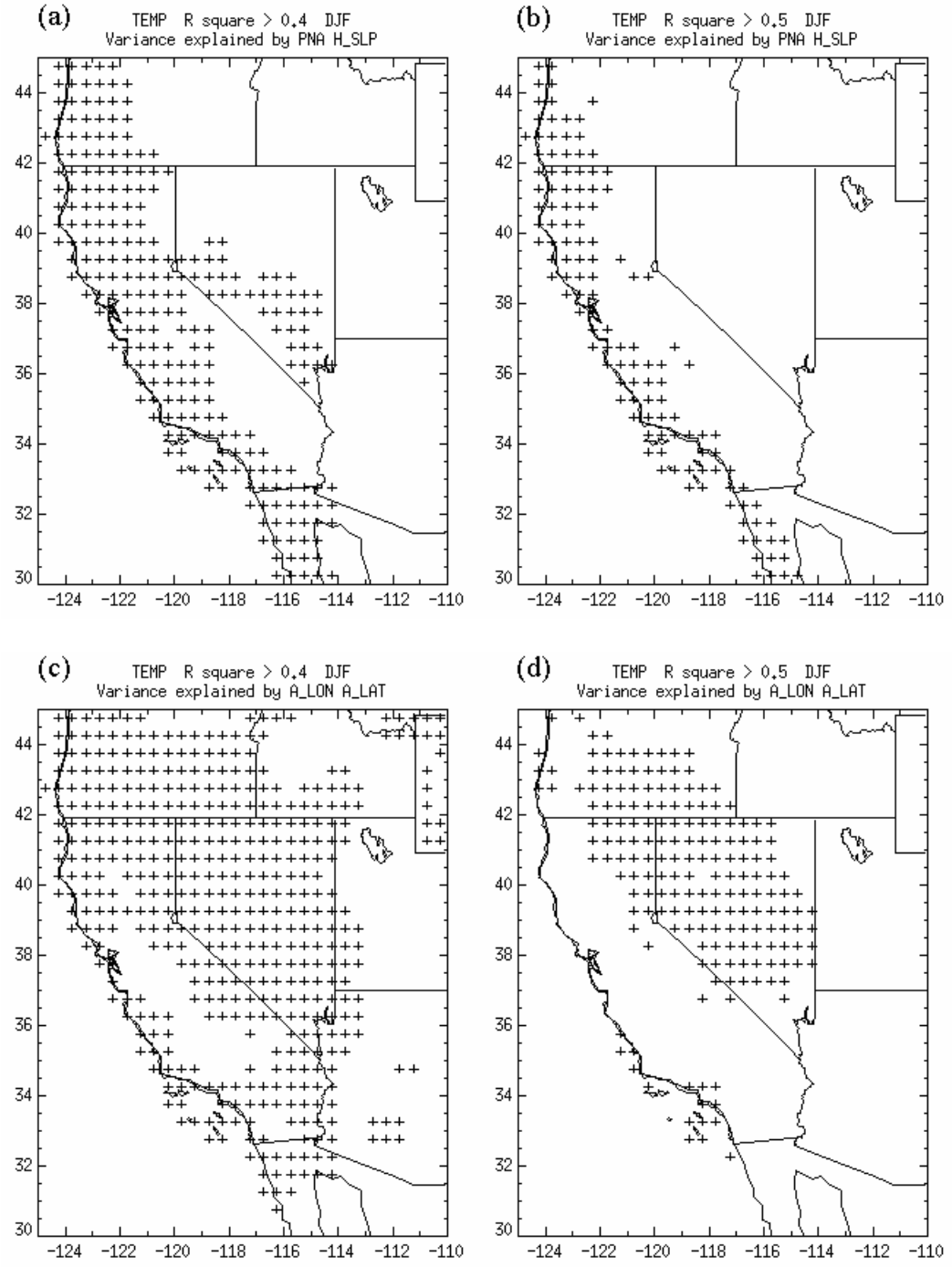

Figure 3.13: Variance of U.S. west coast wintertime (DJFM) temperature explained by (a) PNA and Hawaiian High pressure, variance values higher than 0.4 are marked with cross. (b) same as (a) but with a threshold of 0.5 for variance. (c) Aleutian Low longitude and latitude, values higher than 0.4 are marked with cross. (d) same as (c) but with a threshold of 0.5 for variance.

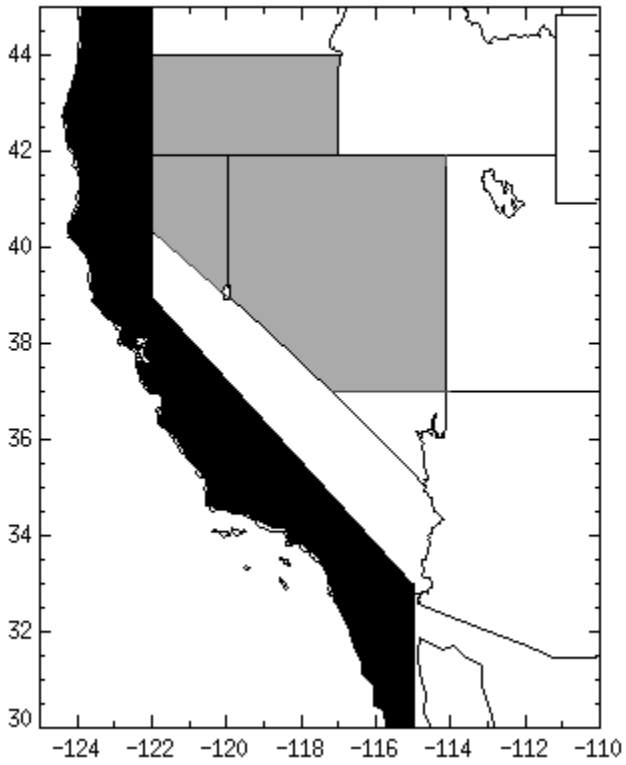

Figure 3.14: Definition of U.S. west coast and Nevada region for area averaged wintertime temperature regression calculation.

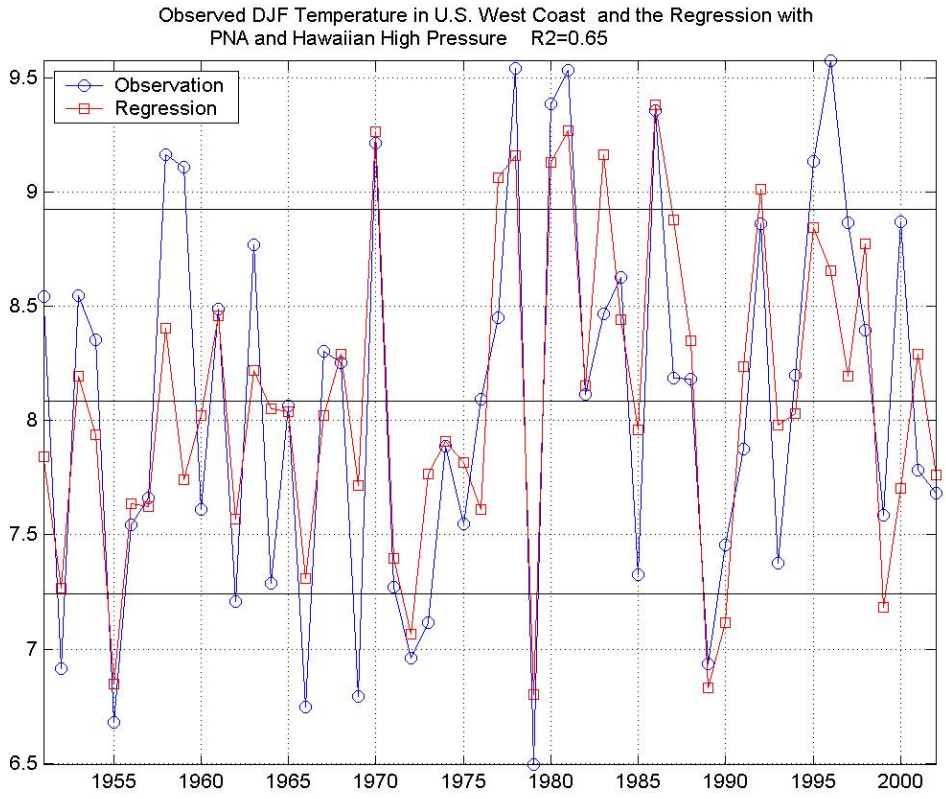

Figure 3.15a: Observed wintertime (DJF) temperature and regression. U.S. west coast, regression with PNA and Hawaiian High pressure.

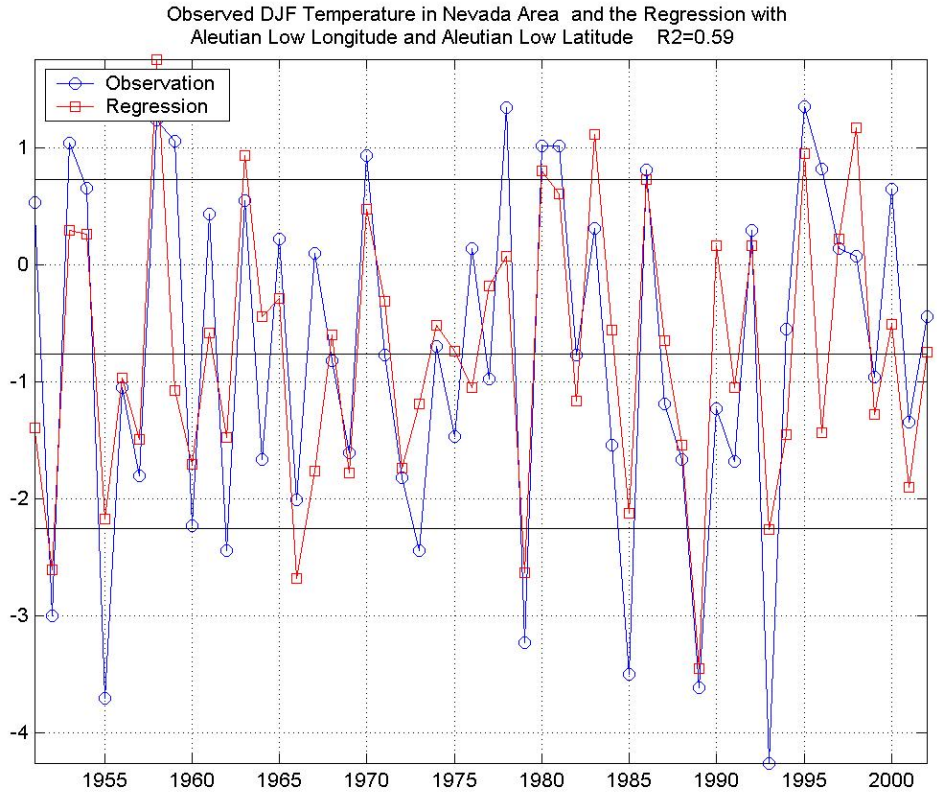

Figure 3.15b: Continued. Observed wintertime (DJF) temperature and regression. Nevada area, regression with Aleutian Low longitude and latitude.

Indices	Variance		
	DJF	**DJFM**	**NDJFM**
Hawaiian high latitude and Aleutian Low pressure	0.33	0.40	0.37
Hawaiian high latitude and Aleutian Low longitude	0.35	0.40	0.37
Hawaiian high latitude and PNA	0.32	0.41	0.37
Hawaiian high latitude	0.32	**0.39**	0.36
Aleutian Low pressure	0.06	0.11	0.08
Aleutian Low longitude	0.21	0.17	0.07
PNA	0.05	0.15	0.10

Table 4.1 Variances from area averaged wintertime Alaska precipitation regression and from single indices only.

Indices	Variance		
	DJF	**DJFM**	**NDJFM**
Hawaiian high pressure and Hawaiian high latitude	0.45	0.46	**0.47**
Hawaiian high pressure and Hawaiian high longitude	0.38	0.41	0.39
Hawaiian high pressure and SOI	0.30	0.35	0.30
Hawaiian high pressure	0.27	0.31	0.28
Hawaiian high latitude	0.18	0.24	0.24
Hawaiian high longitude	0.10	0.11	0.11
SOI	0.11	0.11	0.06

Table 4.2 Variances from area averaged wintertime California precipitation regression and from single indices only.

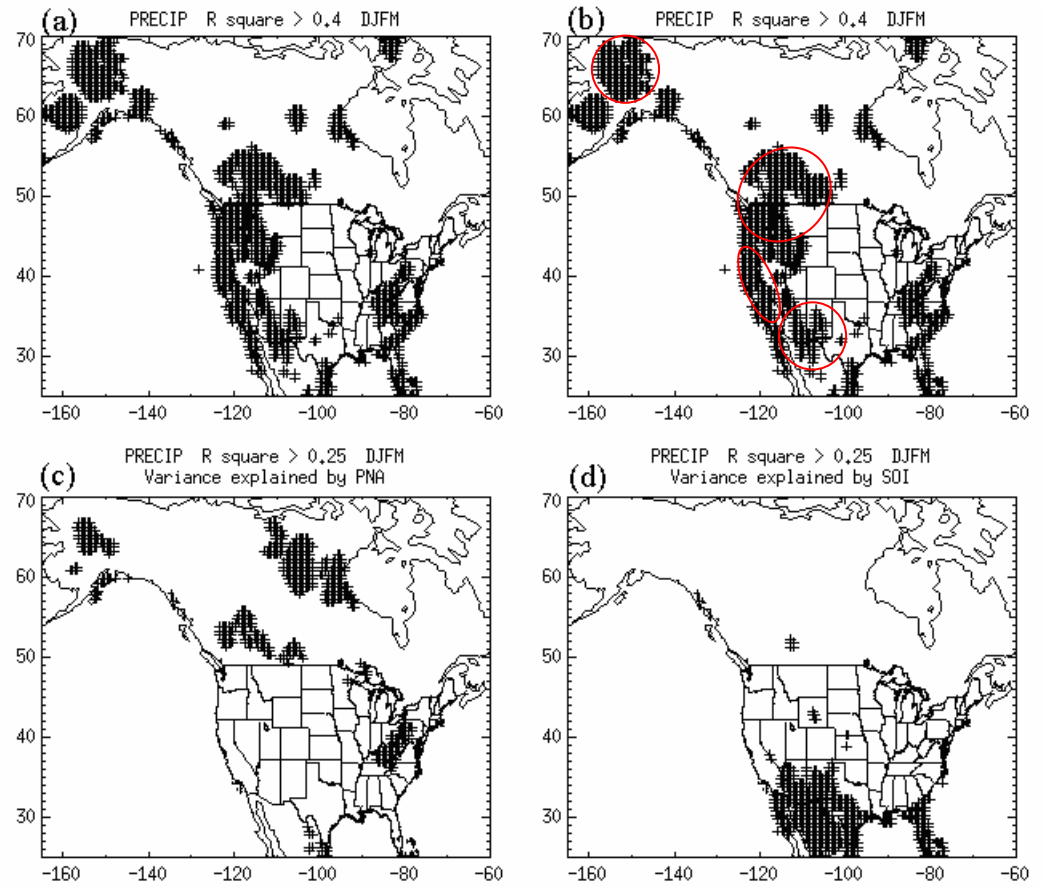

Figure 4.1: (a) North American wintertime (DJFM) precipitation regression with COA indices including Aleutian Low latitude, longitude, sea level pressure, Hawaiian High latitude, longitude, sea level pressure, PNA, and SOI index. (b) same as (a) with major variance distributions marked out in red circles. (c) wintertime (DJFM) precipitation variance explained by PNA only. (d) wintertime (DJFM) precipitation variance explained by SOI only. Variance values higher than 0.4 are marked with cross in (a) and (b). Variance values higher than 0.25 are marked with cross in (c) and (d).

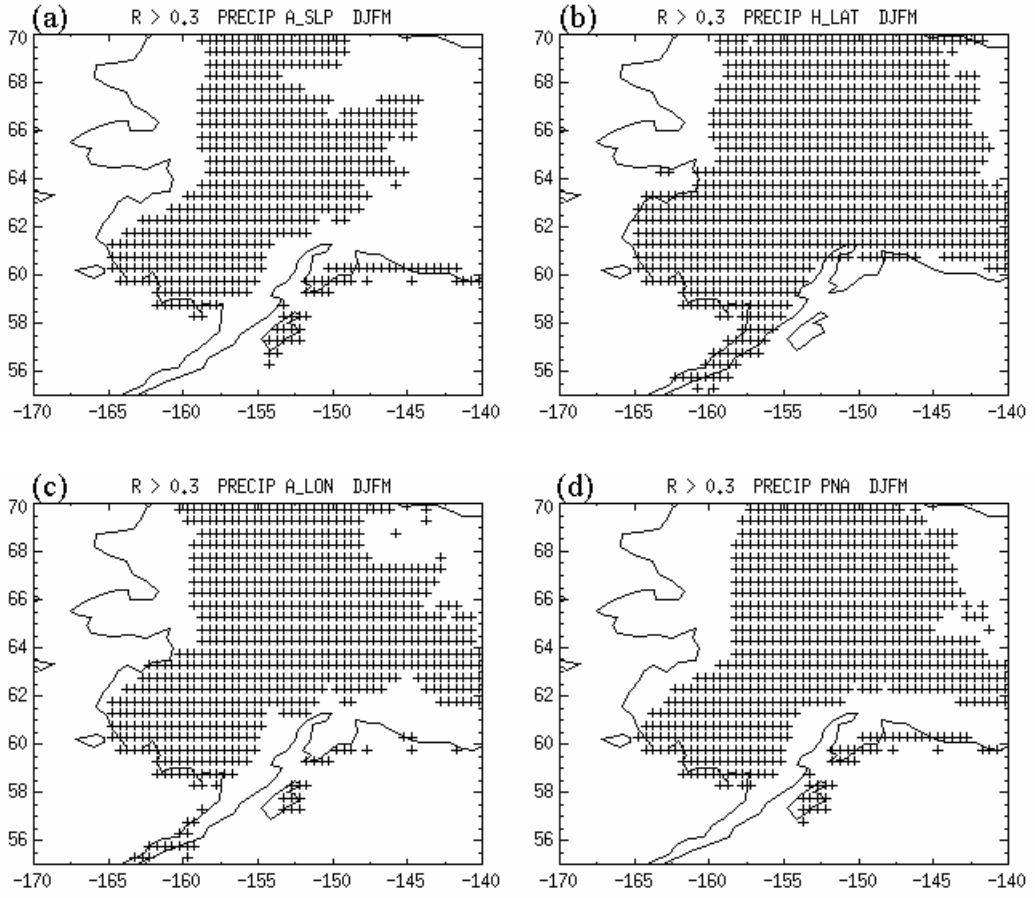

Figure 4.2: Correlations maps between Alaska wintertime (DJFM) precipitation and COA indices. Grid points where absolute value of correlation coefficient higher than 0.3 are marked with cross. COA indices including: (a) Aleutian Low pressure, (b) Hawaiian High latitude, (c) Aleutian Low longitude, (d) PNA.

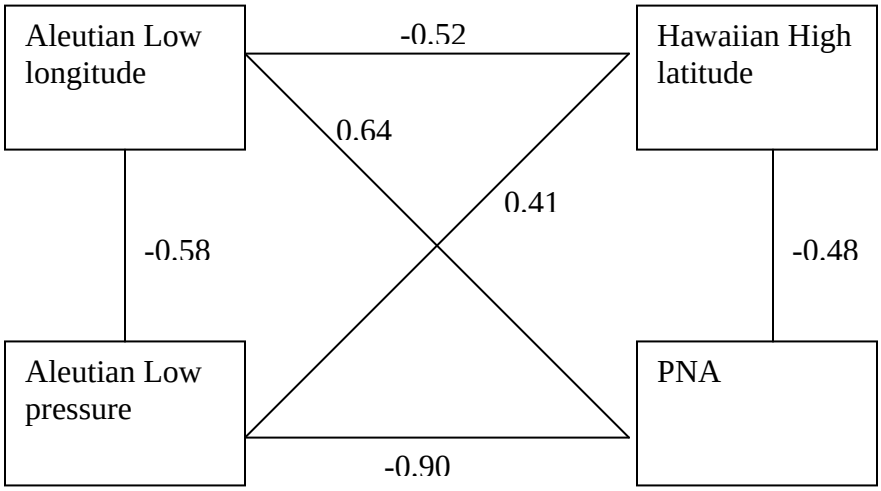

Figure 4.3: Pearson's correlation coefficients between wintertime (DJFM) Aleutian Low longitude, and Aleutian Low pressure, Hawaiian High latitude, and PNA.

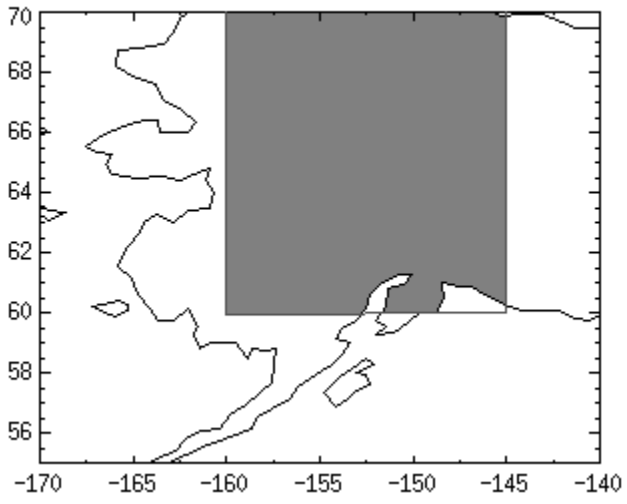

Figure 4.4: Definition of Alaska for area averaged wintertime precipitation regression calculation.

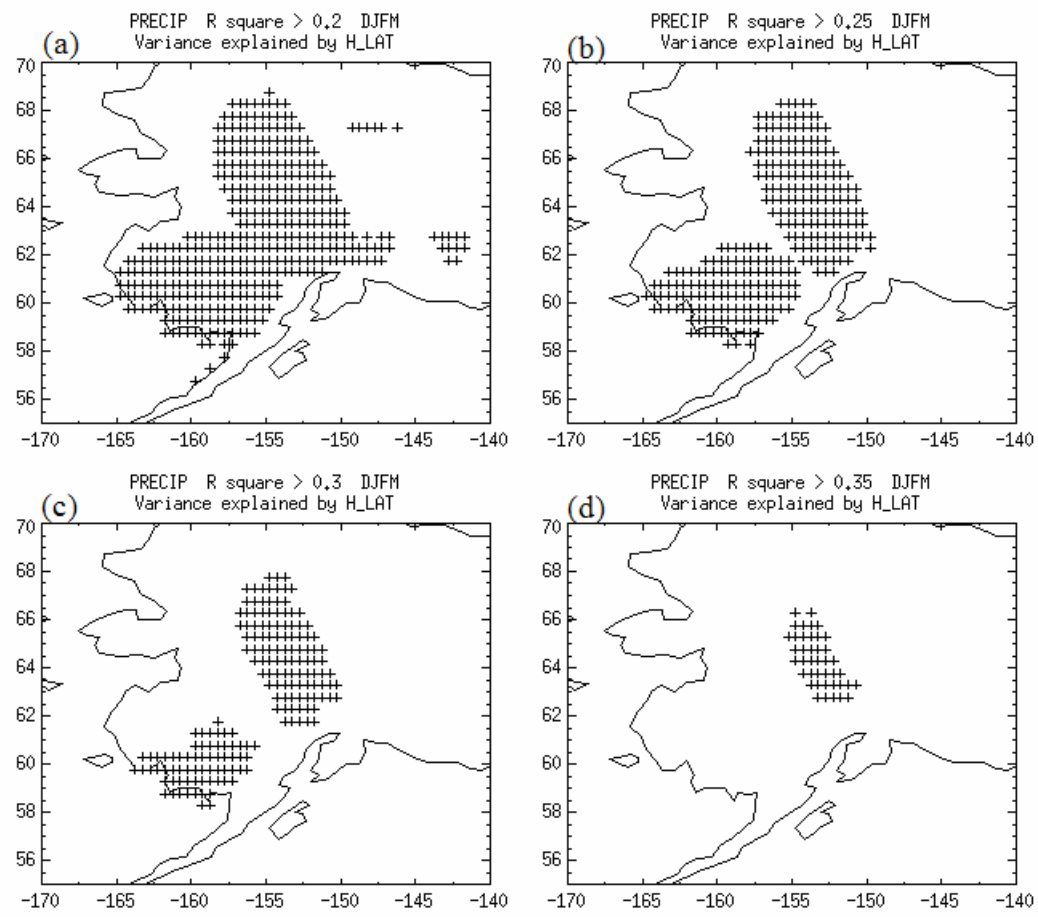

Figure 4.5: Variance of Alaska wintertime (DJF) precipitation explained by Hawaiian High latitude. Grid points are marked with cross if higher than (a) 0.2, (b) 0.25, (c) 0.3, (d) 0.35.

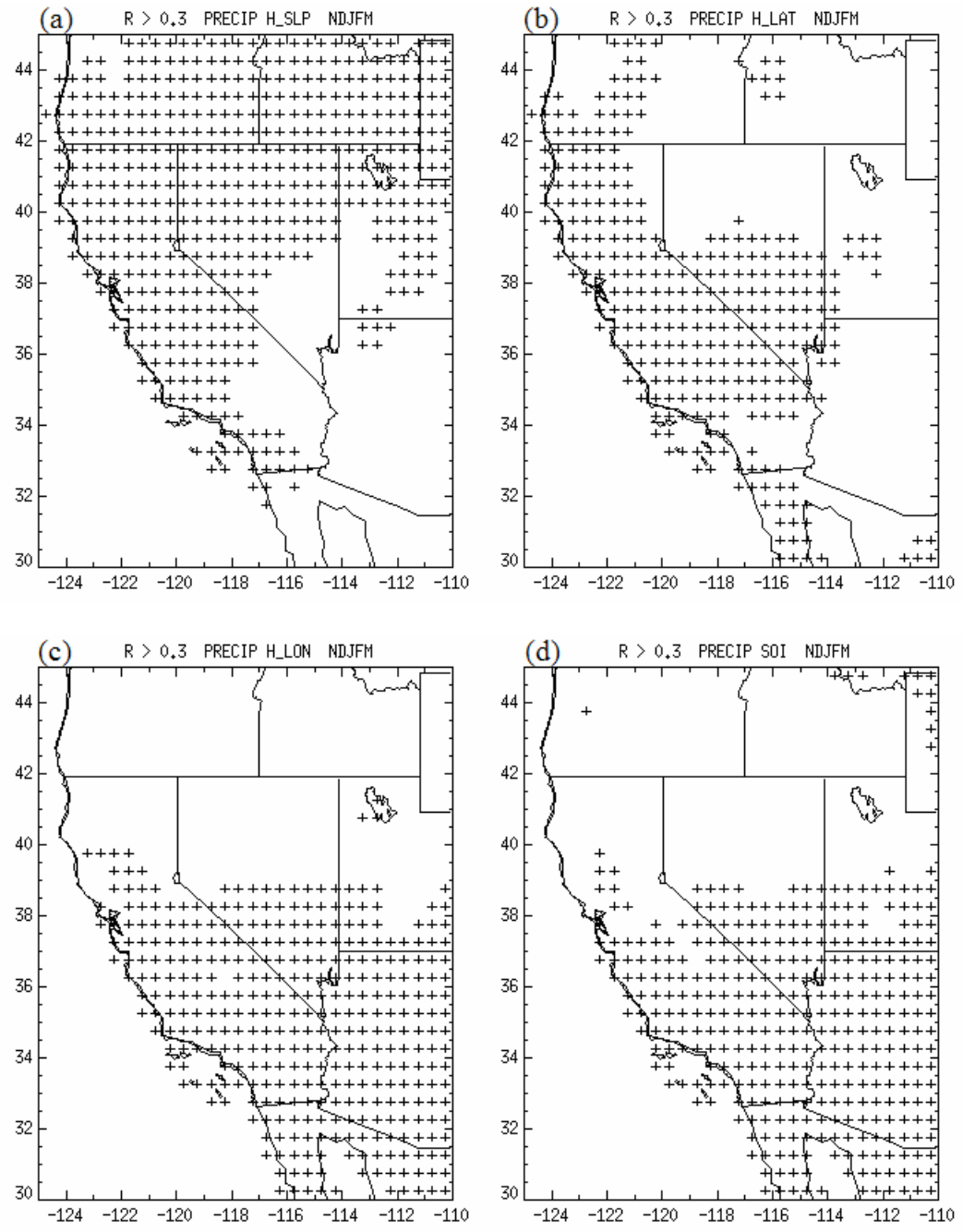

Figure 4.6: Variance of U.S. west coast wintertime (NDJFM) precipitation explained by (a) Hawaiian High pressure, (b) Hawaiian High latitude, (c) Hawaiian High longitude, (d) SOI. Grid points are marked with cross if absolute value is higher than 0.3.

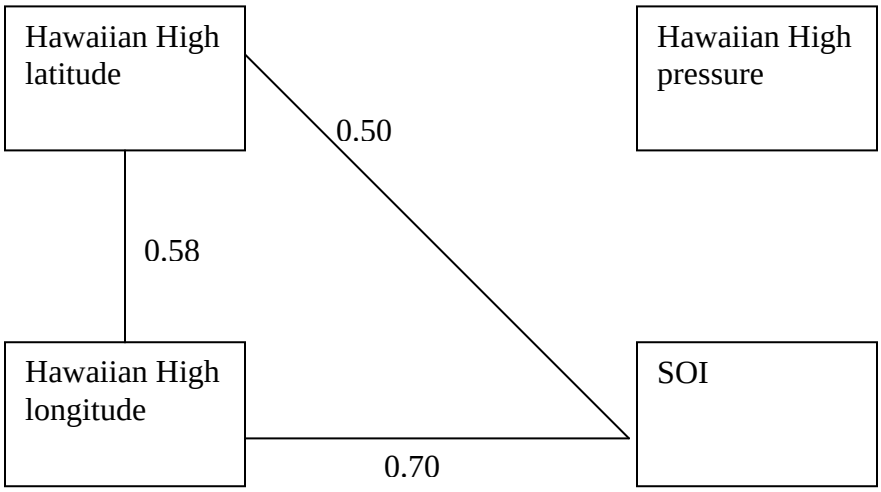

Figure 4.7: Pearson's correlation coefficients between wintertime (NDJFM), Hawaiian High pressure, Hawaiian High latitude, Hawaiian High longitude, and SOI.

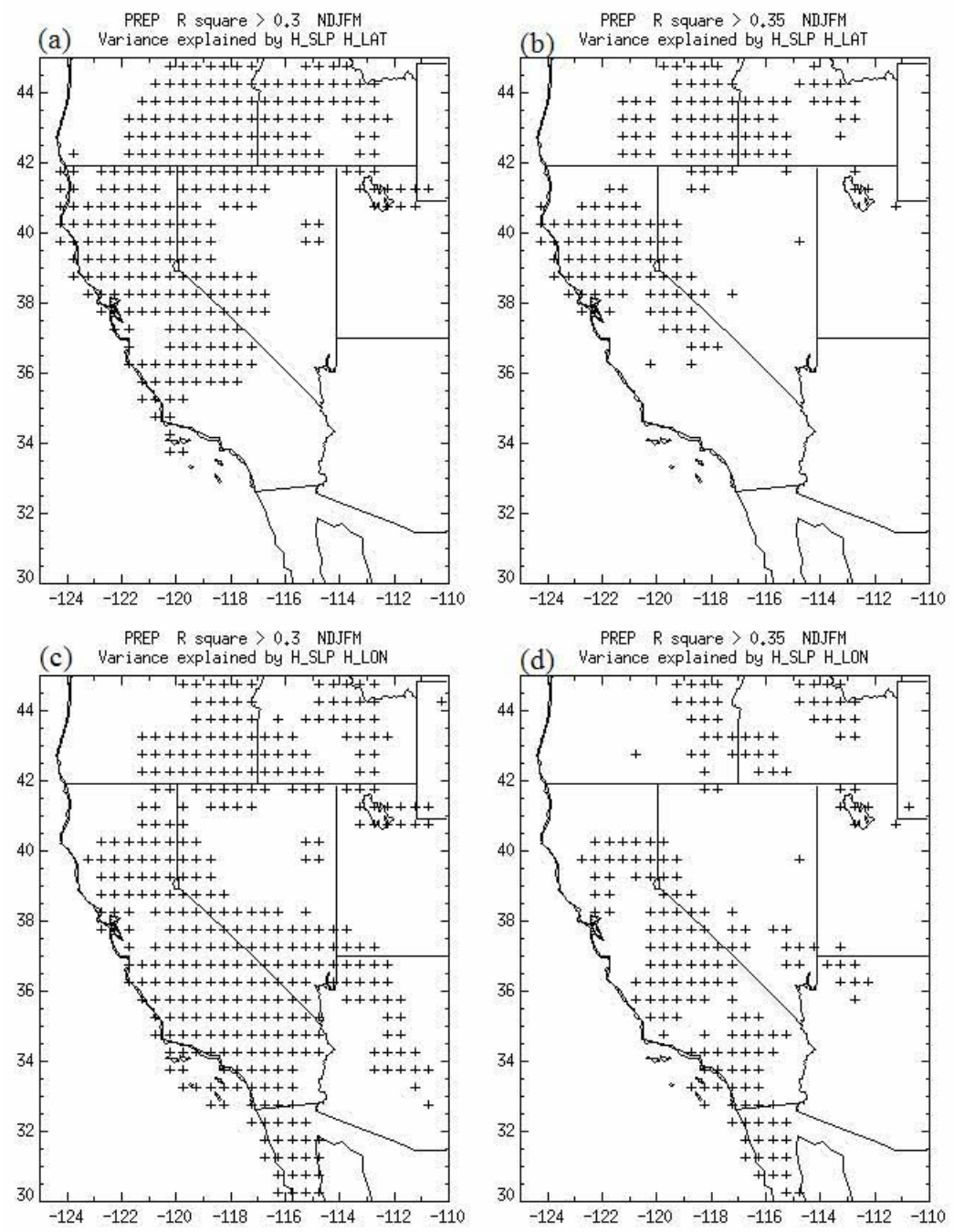

To be continued in next page.

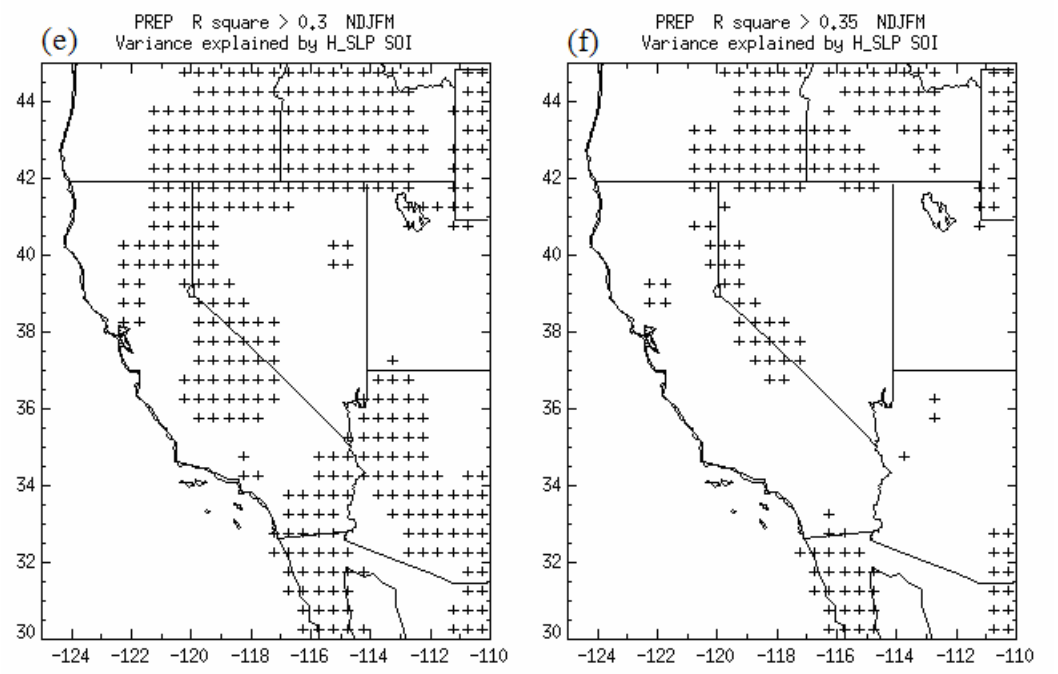

Figure 4.8: Variance of U.S. west coast wintertime (NDJFM) precipitation explained by (a) Hawaiian High pressure and latitude, values higher than 0.3 are marked with cross. (b) same as (a) but with a threshold value of 0.35 for variance mark. (c) Hawaiian High pressure and longitude, values higher than 0.3 are marked with cross. (d) same as (c) but with a threshold value of 0.35 for variance mark. (e) Hawaiian High pressure and SOI, values higher than 0.3 are marked with cross. (f) same as (e) but with a threshold value of 0.35 for variance mark.

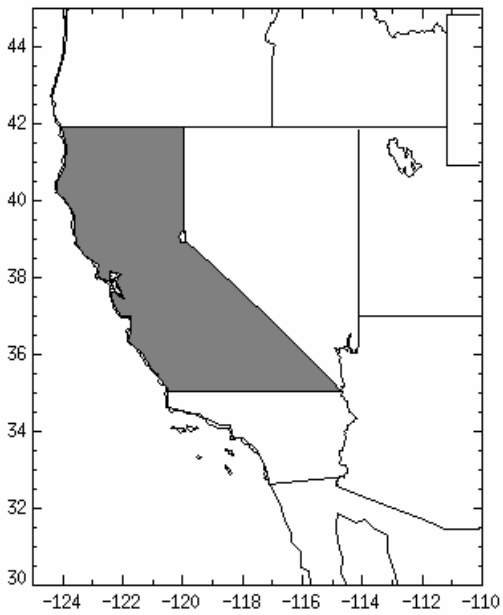

Figure 4.9: Definition of California for area averaged wintertime precipitation calculation.

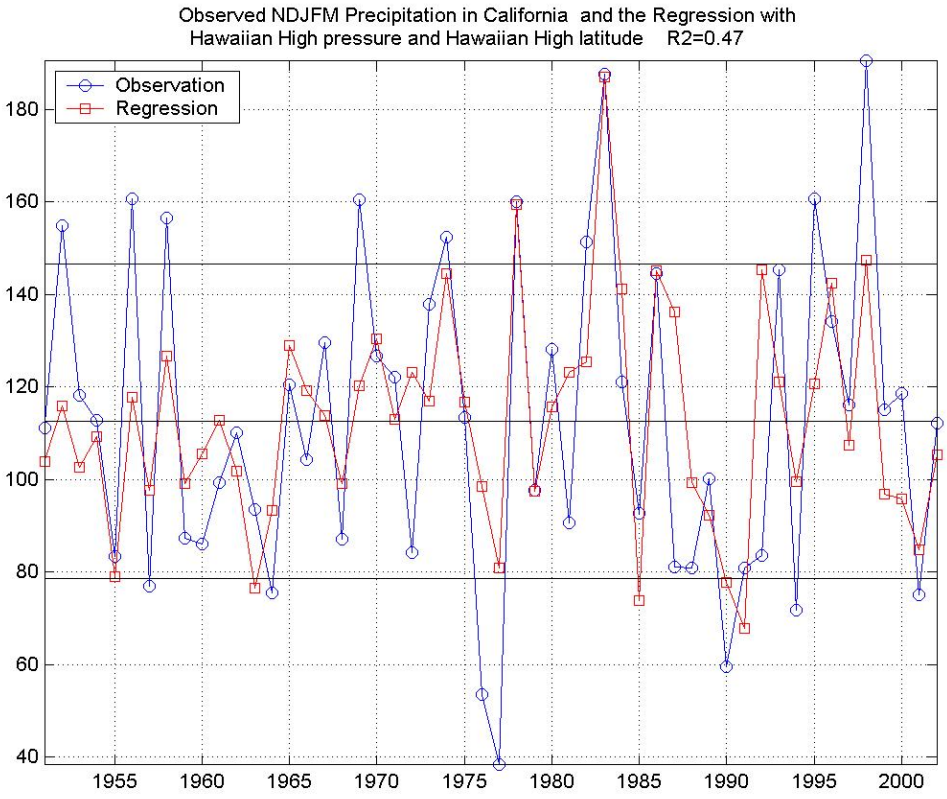

Figure 4.10: Observed wintertime (NDJFM) precipitation and regression in California, regression with Hawaiian High pressure and latitude.

Variable	Region	Indices	Average	Positive years	Negative years
Temperature	U.S. west coast	PNA, H_SLP	DJF	1961, 1964, 1970, 1977, 1978, 1980, 1981, 1983, 1987	1952, 1955, 1957, 1964, 1972, 1979, 1989, 1999
Temperature	Alaska and Canada	PNA (0.86)	DJFM	1961, 1970, 1977, 1981, 1983, 1986, 1987, 1998	1952, 1955, 1956, 1969, 1972
Precipitation	California	H_SLP, H_LAT	NDJFM	1965, 1973, 1978, 1983, 1986, 1996, 1998	1951, 1953, 1955, 1957, 1963, 1964, 1968, 1985, 1991, 1999
Precipitation	Alaska	H_LAT (0.63)	DJFM	1957, 1963, 1968, 1969, 1985, 1989	1953, 1973, 1974, 1978, 1983, 1987, 1992, 1998

Table 5.1: Years used for composite analysis in each regression & correlation case. Positive years are years in which the indices' phase is in favor of positive anomalies in temperature or precipitation. Negative years are years in which the indices' phase is in favor of negative anomalies in temperature or precipitation.

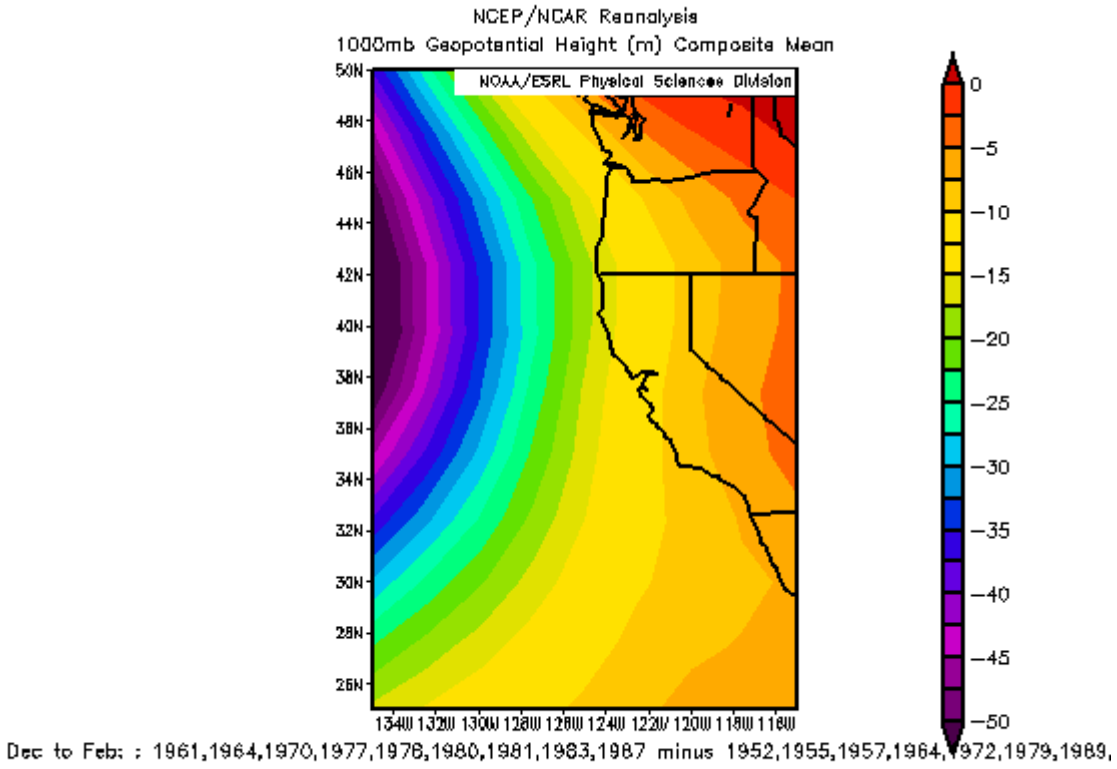

Figure 5.1: 1000mb geopotential height composite associated with indices' phases in favor of high temperature in U.S. west coast. Indices used in this case are: PNA and Hawaiian High pressure.

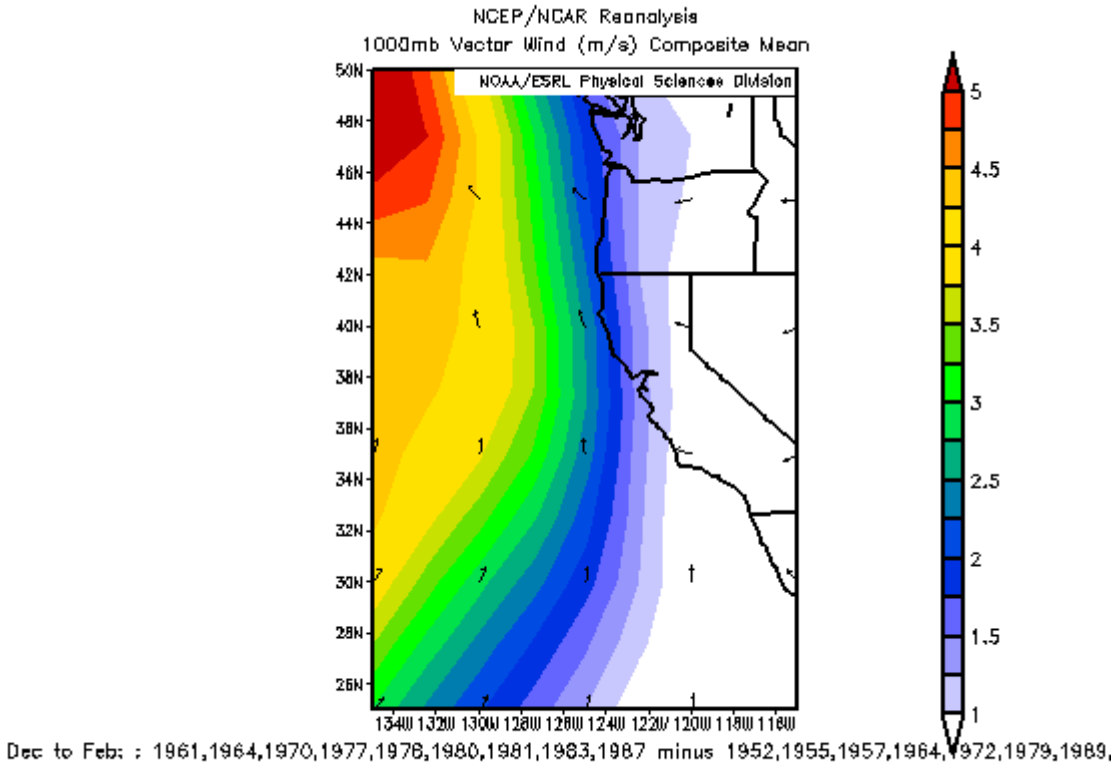

Figure 5.2: 1000mb vector wind composite associated with indices' phases in favor of high temperature in U.S. west coast. Indices used in this case are: PNA and Hawaiian High pressure.

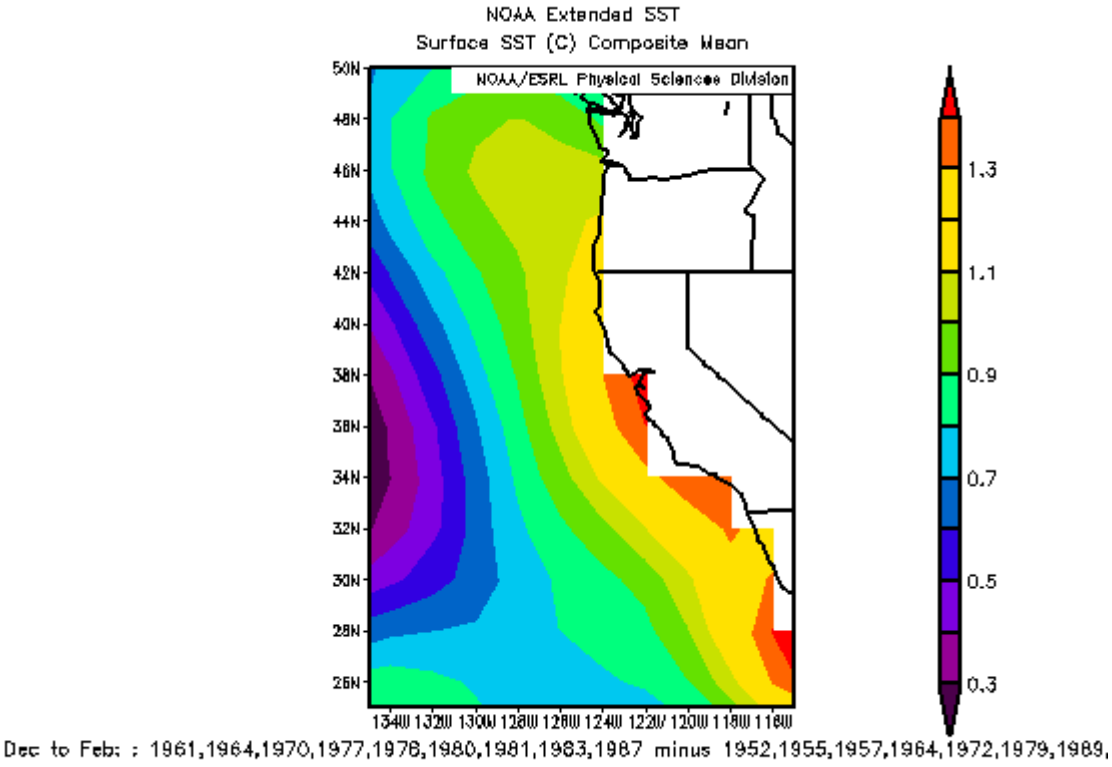

Figure 5.3: Surface SST composite associated with indices' phases in favor of high temperature in U.S. west coast. Indices used in this case are: PNA and Hawaiian High pressure.

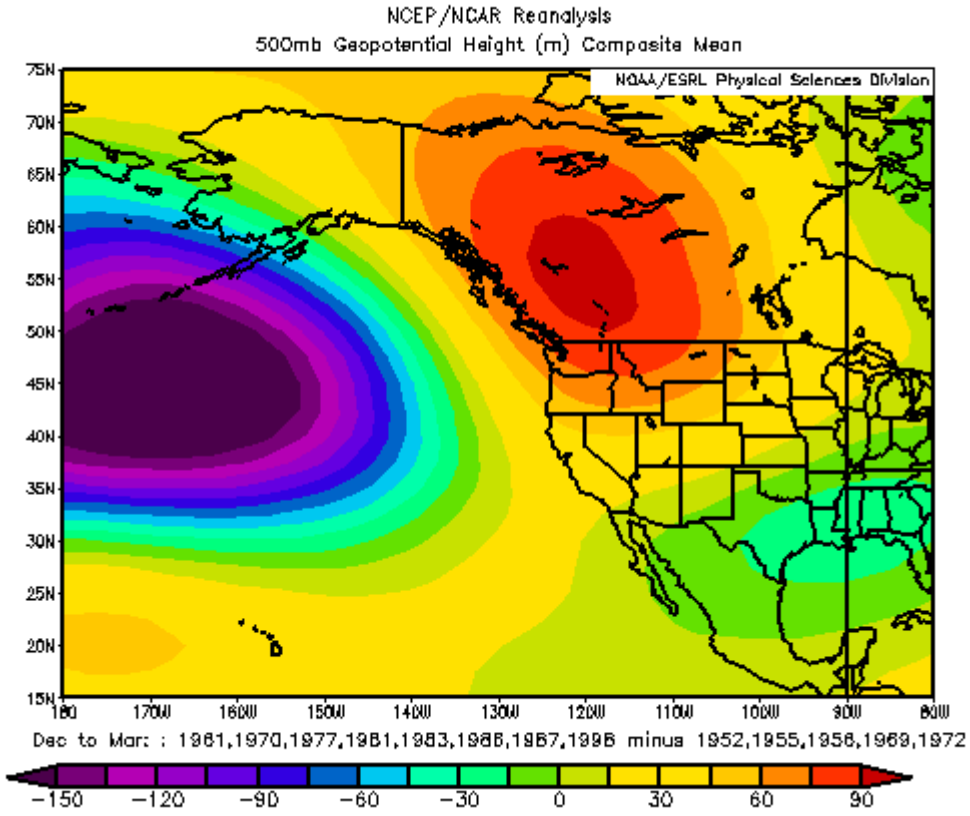

Figure 5.4: 500mb geopotential height composite associated with PNA phases in favor of high temperature in Alaska and west Canada.

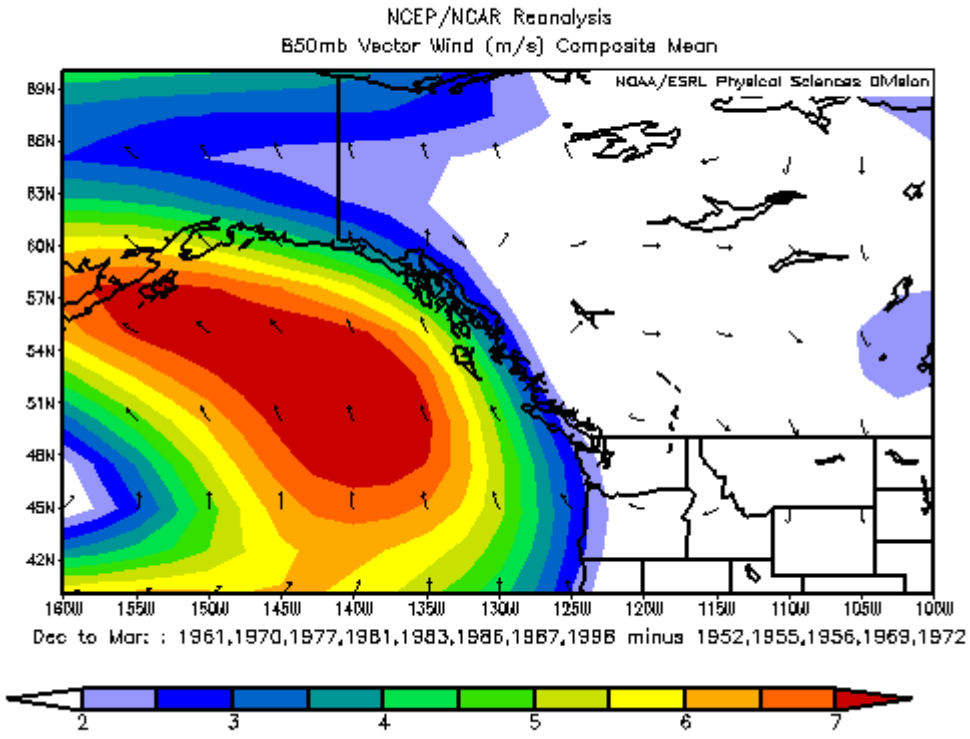

Figure 5.5: 850mb vector wind composite associated with PNA phases in favor of high temperature in Alaska and west Canada.

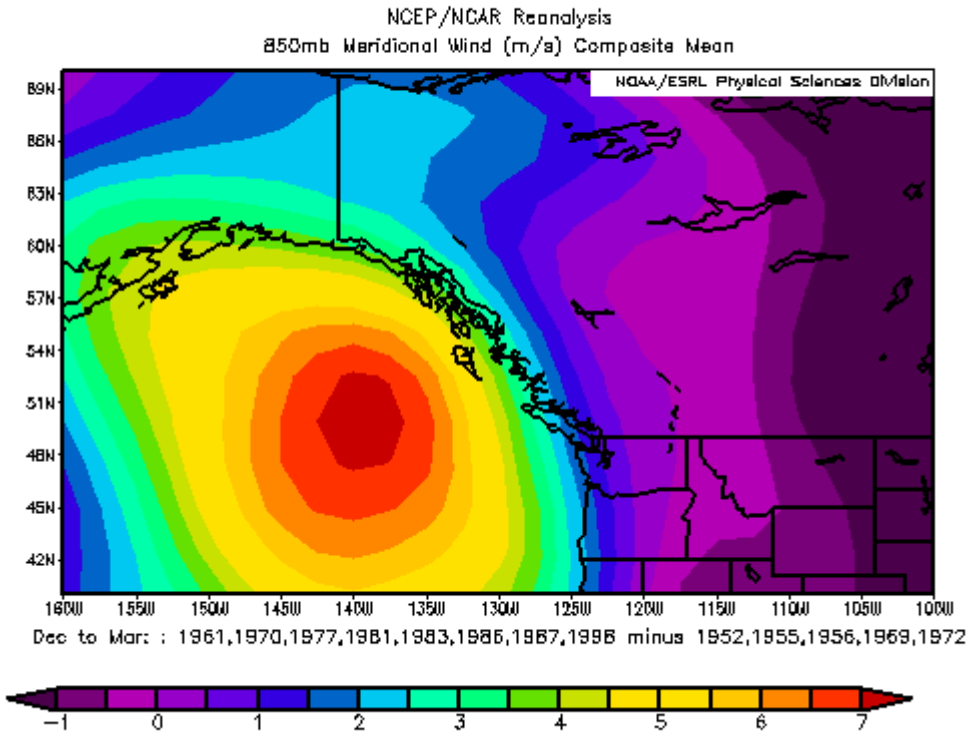

Figure 5.6: 850mb meridional wind composite associated with PNA phases in favor of high temperature in Alaska and west Canada.

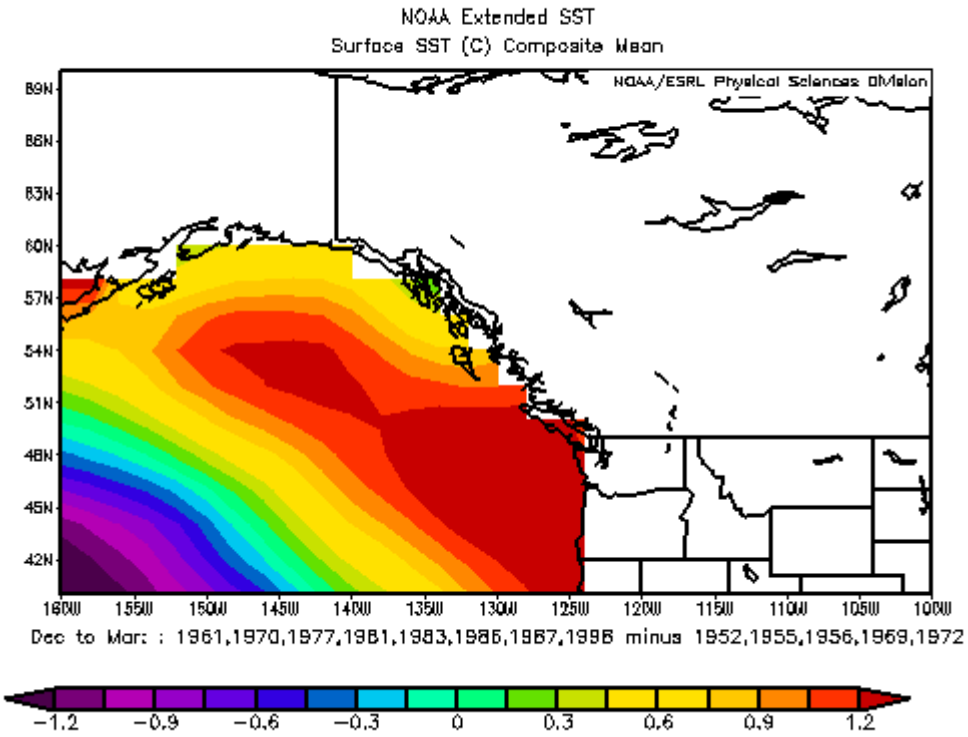

Figure 5.7: Surface SST composite associated with PNA phases in favor of high temperature in Alaska and west Canada.

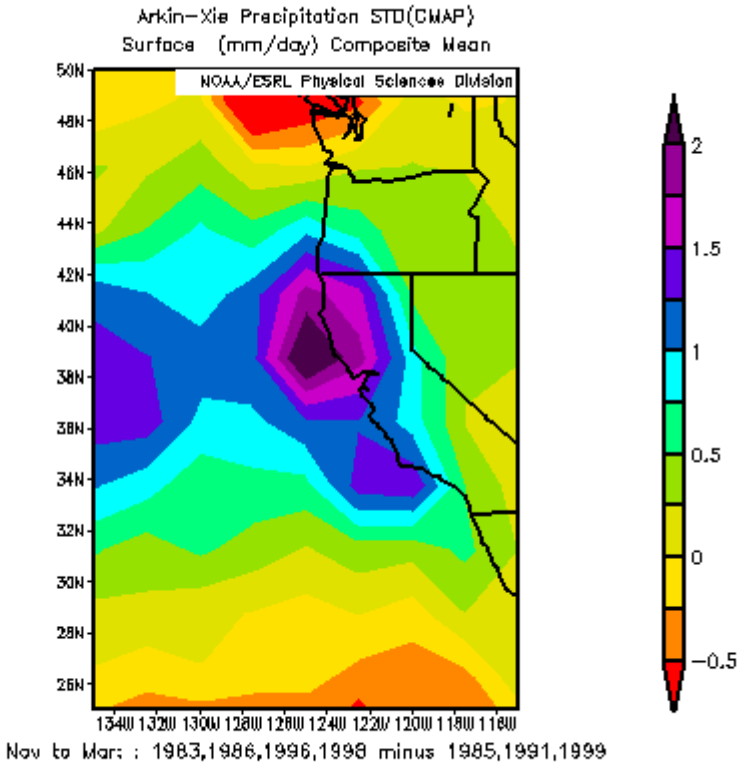

Figure 5.8: Observed precipitation composite associated with indices' phases in favor of high precipitation in California. Indices used in this case are: Hawaiian High pressure and latitude.

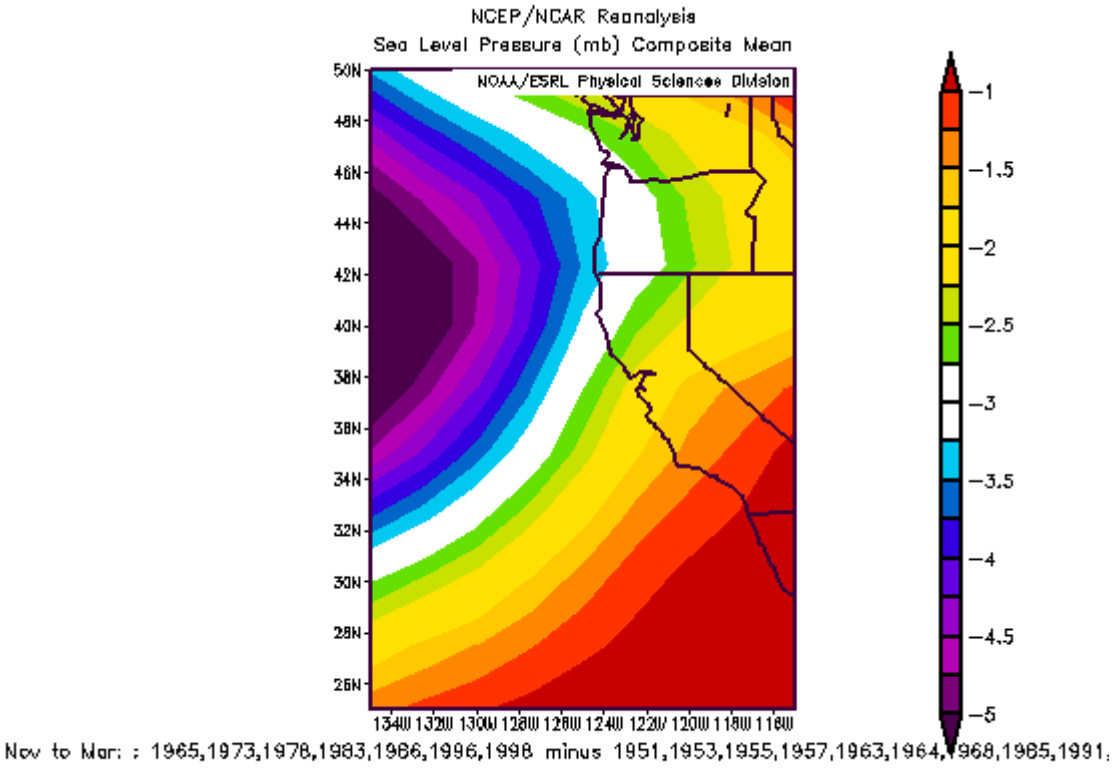

Figure 5.9: Sea level pressure composite associated with indices' phases in favor of high precipitation in California. Indices used in this case are: Hawaiian High pressure and latitude.

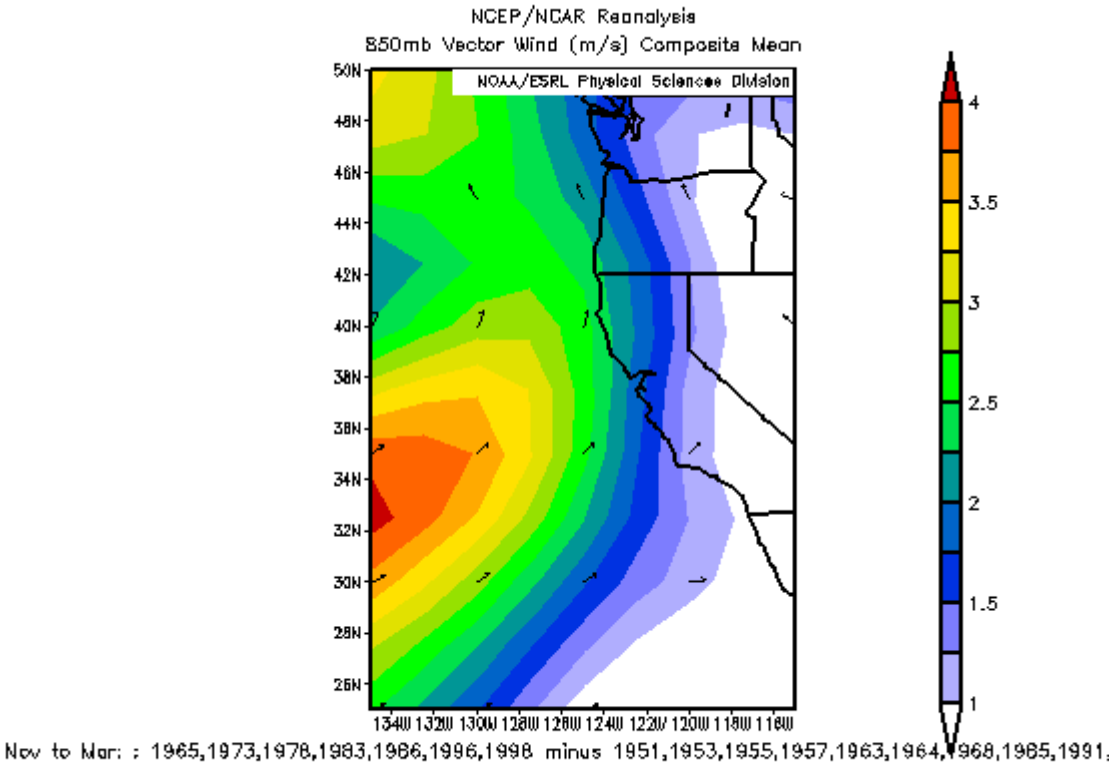

Figure 5.10: 850mb vector wind composite associated with indices' phases in favor of high precipitation in California. Indices used in this case are: Hawaiian High pressure and latitude.

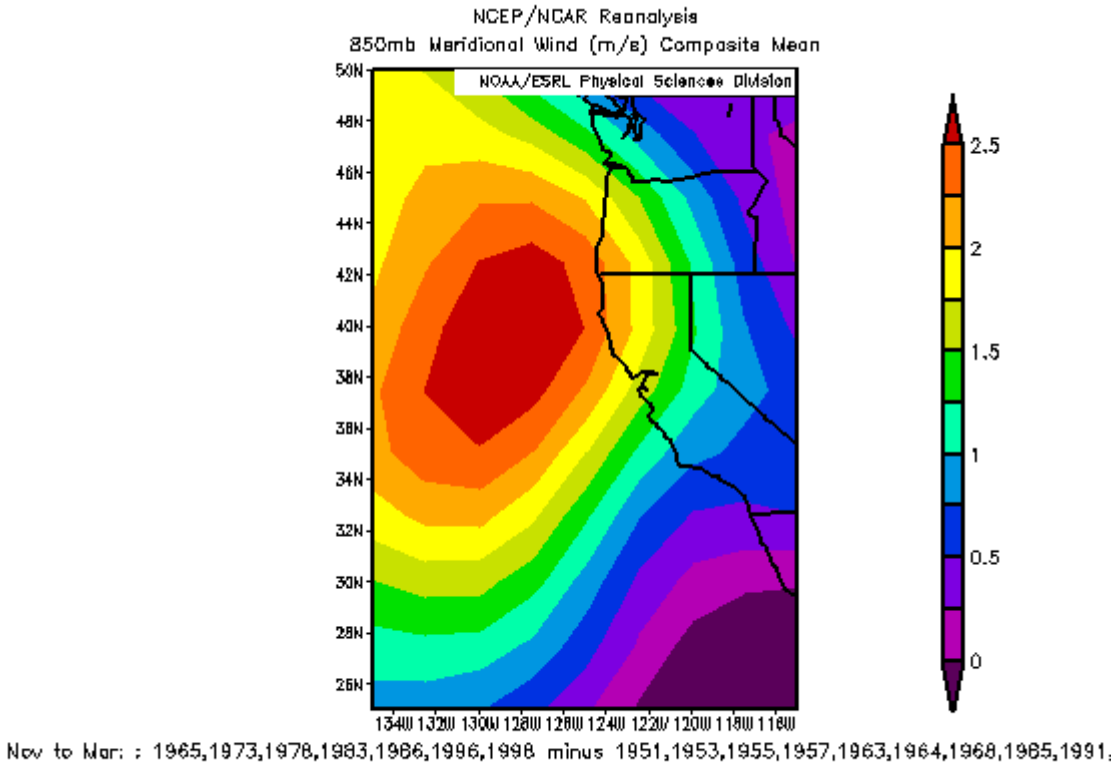

Figure 5.11: 850mb meridional wind composite associated with indices' phases in favor of high precipitation in California. Indices used in this case are: Hawaiian High pressure and latitude.

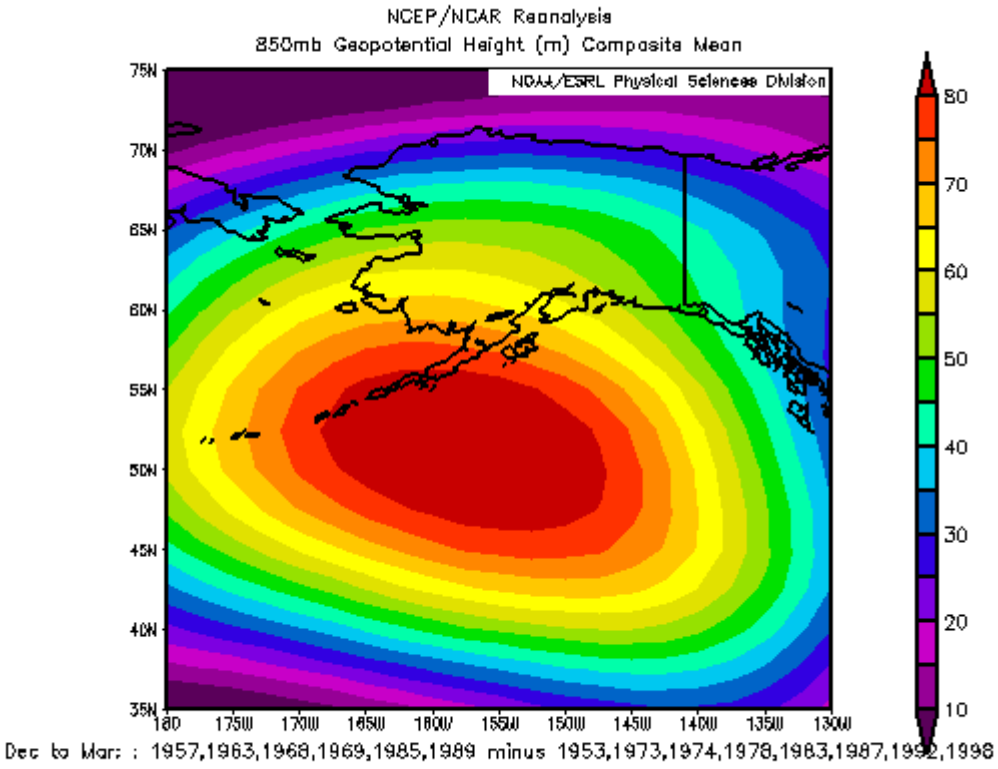

Figure 5.12: 850mb geopotential height composite associated with Hawaiian High latitude's phases in favor of high precipitation in Alaska.

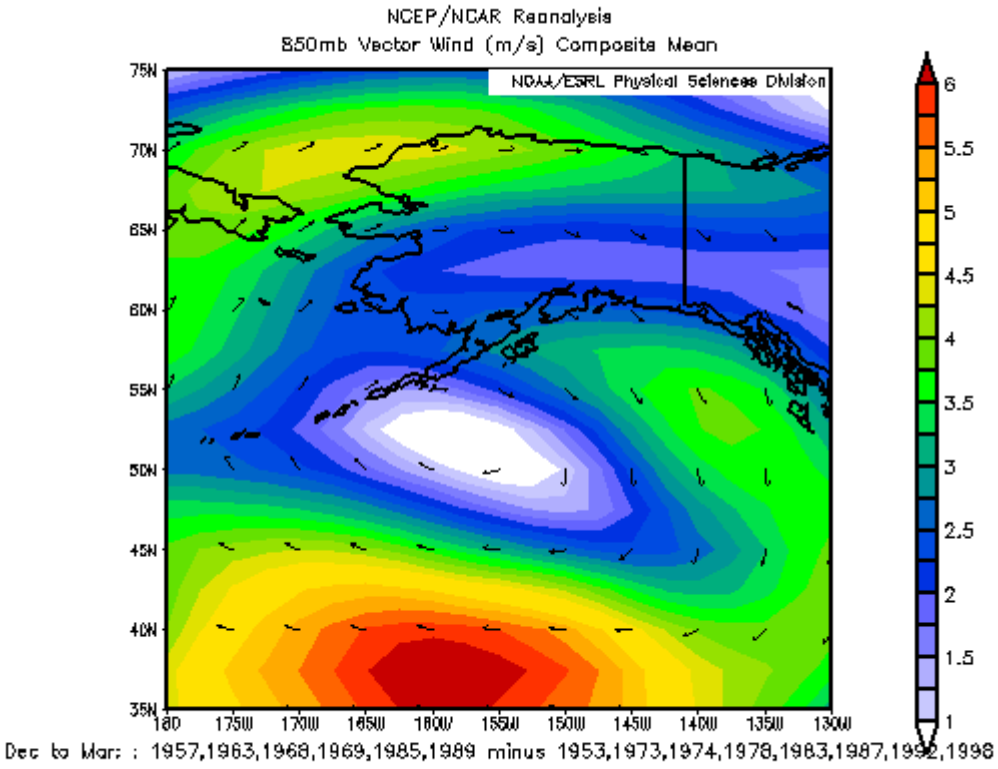

Figure 5.13: 850mb vector wind composite associated with Hawaiian High latitude's phases in favor of high precipitation in Alaska.

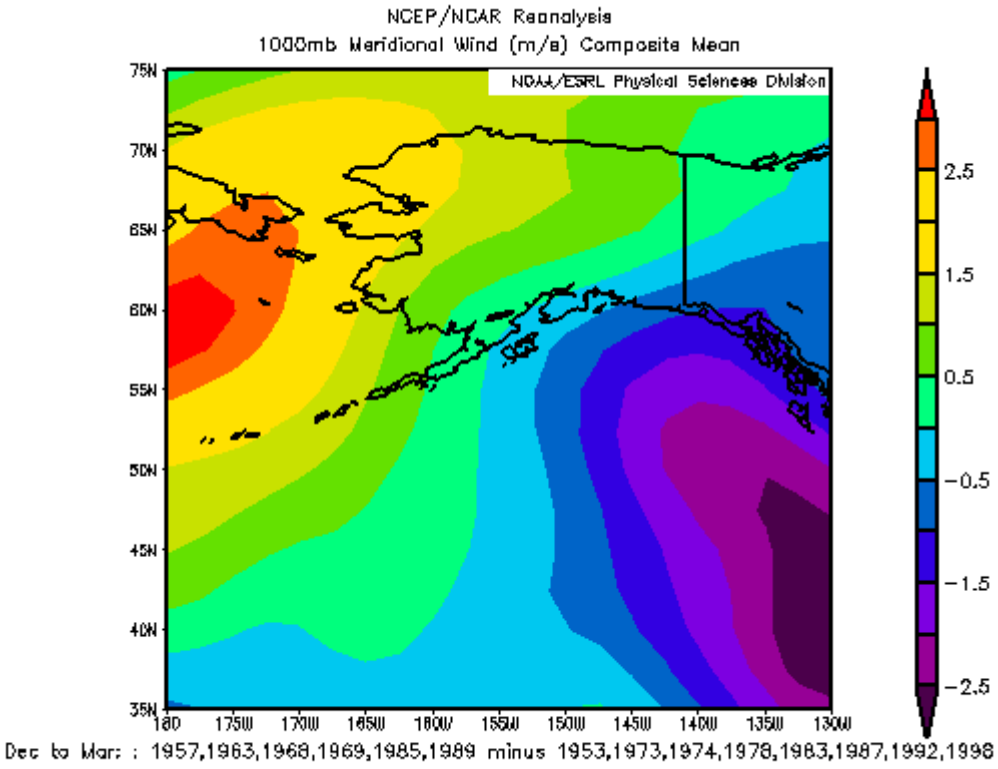

Figure 5.14: 1000mb meridional wind composite associated with Hawaiian High latitude's phases in favor of high precipitation in Alaska.

References

Bakalian, F.M., S. Hameed, R. Pickart (2006) Influence of the Icelandic Low Latitude on the frequency of Greenland Tip Jet Events: Implications for Irminger Sea convection. Journ. Geophys. Res. (oceans).

Barnston, A.G., and R.E. Livezey, 1987: Classification, Seasonality and Persistence of Low-Frequency Atmospheric Circulation Patterns. Mon. Wea. Rev., 115, 1083–1126.

Brown, D. P., and A. C. Comrie (2004), A winter precipitation 'dipole' in the western United States associated with multidecadal ENSO variability, Geophys. Res. Lett., 31, L09203, doi:10.1029/2003GL018726.

Cayan, D. R., and K. T. Redmond, 1994: ENSO influences on atmospheric circulation and precipitation in the western United States. Proc. 10th Annual Pacific Climate (PACLIM) Workshop, Pacific Grove, CA, California Department of Water Resources, 5–26.

Chen, T.C., J.M. Chen, and C.K. Wikle, 1996: Interdecadal Variation in U.S. Pacific Coast Precipitation over the Past Four Decades. Bull. Amer. Meteor. Soc., 77, 1197–1205.

Croke, M.S., R.D. Cess, S. Hameed (1999) Regional cloud cover change associated with global climate change: Case studies for three regions of the United States. J. Climate, 12, 2128-2134.

Dettinger, M. D., D. R. Cayan, H. F. Diaz, and D. M. Meko (1998), Northsouth precipitation patterns in western North America on interannual-todecadal timescales, J. Clim., 11, 3095– 3111.

Hameed, S., Shi, W., Boyle, J. and Santer, B., 1995: Investigation of the centers of action in the North Atlantic and North Pacific in the ECHAM AMIP simulation, Proceedings of the First International AMIP Scientific Conference, WCRP-92, WMO/TD-No. 732, 221-226.

Hameed S., and S.A. Piontkovski. 2004. The dominant influence of the Icelandic Low on the position of the Gulf Stream northwall. Geophys.Res.Let.,31, L09303.

Haston, L., and J. Michaelsen, 1994: Long-Term Central Coastal California Precipitation Variability and Relationships to El Niño-Southern Oscillation. J. Climate, 7, 1373–1387.

Haston, L., and J. Michaelsen, 1997: Spatial and Temporal Variability of Southern California Precipitation over the Last 400 yr and Relationships to Atmospheric Circulation Patterns. J. Climate, 10, 1836–1852.

Mitchell, T.P., and W. Blier, 1997: The Variability of Wintertime Precipitation in the Region of California. J. Climate, 10, 2261–2276.

Mitchell T. D. and P. D. Jones. 2005. An improved method of constructing a database of monthly climate observations and associated high-resolution grids. International Journal of Climatology 25, 693-712.

Mo, K.C., and R.W. Higgins, 1998: Tropical Influences on California Precipitation. J. Climate, 11, 412–430.

Piontkovski, S., and S.Hameed (2002) Precursors of Copepod Abundance in the Gulf of Main in Atmospheric Centers of Action and Sea Surface Temperature. The Global Atmosphere and Ocean System, 8, 283-291.

Riemer R., O.M. Doherty, and S. Hameed (2006) On the variability of African dust transport across the Atlantic. Geophys. Res. Lett., 33, L13814.

Wallace, J.M., and D.S. Gutzler, 1981: Teleconnections in the Geopotential Height Field during the Northern Hemisphere Winter. Mon. Wea. Rev., 109, 784–812.